APL-1, the Alzheimer's Amyloid Precursor Protein in *Caenorhabditis elegans*, Modulates Multiple Metabolic Pathways Throughout Development

Collin Y. Ewald,*,† Daniel A. Raps,† and Chris Li*,†,1
*Graduate Center, City University of New York, New York, New York 10016 and †Department of Biology, City College of New York, New York, New York 10031

ABSTRACT Mutations in the *amyloid precursor protein* (*APP*) gene or in genes that process APP are correlated with familial Alzheimer's disease (AD). The biological function of APP remains unclear. APP is a transmembrane protein that can be sequentially cleaved by different secretases to yield multiple fragments, which can potentially act as signaling molecules. *Caenorhabditis elegans* encodes one APP-related protein, APL-1, which is essential for viability. Here, we show that APL-1 signaling is dependent on the activity of the FOXO transcription factor DAF-16 and the nuclear hormone receptor DAF-12 and influences metabolic pathways such as developmental progression, body size, and egg-laying rate. Furthermore, *apl-1(yn5)* mutants, which produce high levels of the extracellular APL-1 fragment, show an incompletely penetrant temperature-sensitive embryonic lethality. In a genetic screen to isolate mutants in which the *apl-1(yn5)* lethality rate is modified, we identified a suppressor mutation in MOA-1/R155.2, a receptor-protein tyrosine phosphatase, and an enhancer mutation in MOA-2/B0495.6, a protein involved in receptor-mediated endocytosis. Knockdown of *apl-1* in an *apl-1(yn5)* background caused lethality and molting defects at all larval stages, suggesting that *apl-1* is required for each transitional molt. We suggest that signaling of the released APL-1 fragment modulates multiple metabolic states and that APL-1 is required throughout development.

THE cause of Alzheimer's disease (AD) remains unknown. Mutations in several genes, including the amyloid precursor protein (APP), are correlated with inherited forms of AD. Furthermore, a defining feature of AD is large numbers of senile plaques in the brain, and the plaques' major component is a cleavage byproduct of APP. The normal function of APP and its cleavage products is still unclear. Here, we report that the *Caenorhabditis elegans* APP-related protein APL-1 has multiple functions during development, including modulating the insulin pathway. These results indicate that human APP may similarly regulate metabolic processes, such as the insulin pathway.

AD is a neurodegenerative disorder that leads to cognitive decline (Alzheimer's Association 2010). One postmortem criterion in the diagnosis of AD is the presence of senile plaques in AD patients (Kidd 1964; Luse and Smith 1964; Terry *et al.* 1964; Krigman *et al.* 1965). The major component of the senile plaques is the β-amyloid peptide, which is a cleavage fragment of APP (Kang *et al.* 1987). Mutations and duplications of APP have been correlated with familial Alzheimer's disease (Chartier-Harlin *et al.* 1991; Goate *et al.* 1991; Murrell *et al.* 1991; Cabrejo *et al.* 2006; Rovelet-Lecrux *et al.* 2006; Sleegers *et al.* 2006). APP is a single pass transmembrane domain protein (Kang *et al.* 1987), which can be cleaved by either an α- or a β-secretase to release a large extracellular fragment (sAPPα or sAPPβ, respectively); the remaining transmembrane fragment is subsequently cleaved by the γ-secretase to release a small intracellular fragment (APP intracellular domain, AICD) and, in the case of a previous β-secretase cleavage, the β-amyloid peptide (reviewed in Gralle and Ferreira 2007). The biological functions of the cleaved APP fragments, sAPPα/β and AICD, remain unclear. Crystal structures of sAPP revealed a growth-factor–like domain that is conserved and present in all mammalian APP-family members as well

doi: 10.1534/genetics.112.138768
Manuscript received January 18, 2012; accepted for publication March 24, 2012
Supporting information is available online at http://www.genetics.org/content/suppl/2012/03/30/genetics.112.138768.DC1.
[1]Corresponding author: City College of New York, MR-526, 160 Convent Ave., New York, NY 10031. E-mail: cli@sci.ccny.cuny.edu

in *C. elegans* and *Drosophila* orthologs (Rossjohn *et al.* 1999), consistent with a growth factor role reported *in vitro* (reviewed in Mattson 1997; Schmitz *et al.* 2002). Conversely, fragments of sAPPβ can act as a ligand that directly binds death receptor 6 (DR6) to initiate neurodegeneration (Nikolaev *et al.* 2009; Kuester *et al.* 2011). *In vivo* sAPP can act as a co-factor to promote cell proliferation of ventricular zone cells (Caille *et al.* 2004). However, determining the function of APP in mammals is complicated by two functionally redundant proteins, APLP1 and APLP2. In mice, knockout of *APP* leads to mild deficits (Zheng *et al.* 1995), while double knockouts of *APP* and *APLP2* or triple knockouts of *APP*, *APLP1*, and *APLP2* lead to postnatal lethality (Heber *et al.* 2000; Herms *et al.* 2004). The nematode *C. elegans* encodes only one APP-related gene, *apl-1* (Daigle and Li 1993). Like the APP family in mice, *apl-1* has an essential function: knockout of *apl-1* results in larval lethality due to a molting defect during the first to the second larval transition (Hornsten *et al.* 2007; Wiese *et al.* 2010). The molting defect of *apl-1* knockouts is rescued not only by reintroducing an *apl-1* genomic fragment, but also by reintroducing a fragment containing only the APL-1 extracellular domain (Hornsten *et al.* 2007). These results suggest that sAPL-1 acts during early development and is sufficient for viability. Whether sAPL-1 is necessary later in development is unclear.

In *C. elegans* postembryonic developmental programs and progression through larval transitions are influenced by environmental conditions (Tennessen *et al.* 2010; Monsalve *et al.* 2011; for review see Resnick *et al.* 2010). Under favorable conditions, *C. elegans* eggs hatch and develop through four larval stages (L1–L4) before reaching adulthood (Sulston and Horvitz 1977). If no food is present when the eggs hatch, the first larval stage animals halt development and go into an L1 arrest until food becomes present (Baugh and Sternberg 2006). However, if food is limited during the first and second larval stages, L2 worms enter an alternate stage called dauer (Cassada and Russell 1975). Dauer animals can survive in a harsh environment for >3 months and are resistant to heat and various noxious chemicals (Cassada and Russell 1975; Klass and Hirsh 1976; Larsen 1993; Lithgow *et al.* 1995). The activity of the DAF-2 insulin/IGF-1 receptor regulates both L1 arrest and dauer formation (Riddle *et al.* 1981; Vowels and Thomas 1992; Larsen *et al.* 1995; Gems *et al.* 1998). Complete loss of *daf-2* function leads to L1 arrest and lethality (Gems *et al.* 1998), whereas reduced DAF-2 activity can keep newly hatched eggs in L1 arrest, even when food is present (Gems *et al.* 1998; Baugh and Sternberg 2006). For L1 arrest either by starvation or reduced *daf-2* activity, activity of the DAF-16 FOXO transcription factor is required (Baugh and Sternberg 2006). DAF-2 insulin/IGF-1 receptor signaling negatively regulates DAF-16 FOXO activity by phosphorylation of DAF-16, thereby limiting its localization to the cytoplasm (Lin *et al.* 1997; Ogg *et al.* 1997).

Developmental programs activated by environmental conditions are integrated with a complex regulatory pathway of heterochronic genes that control the timing of stage-specific developmental programs to allow smooth transitioning into the different larval stages or adulthood (Monsalve *et al.* 2011; for review see Resnick *et al.* 2010). For the last molt of L4 to adulthood, for instance, the microRNA (miRNA) *let-7* binds the 3′-UTR of mRNA from the heterochronic genes *lin-41* (Slack *et al.* 2000) and *hbl-1* (Abrahante *et al.* 2003) and the *daf-12* nuclear hormone receptor (NHR) gene (Antebi *et al.* 2000; Grosshans *et al.* 2005) to prevent their translation. The *let-7* targets, *daf-12* and *hbl-1*, in turn negatively feed back to regulate *let-7* (Bethke *et al.* 2009; Hammell *et al.* 2009; Roush and Slack 2009). During late L4 development, *let-7* also regulates expression of *apl-1* via *hbl-1*, *lin-41*, *lin-42* heterochronic, and *nhr-25* NHR genes (Niwa *et al.* 2008; Hada *et al.* 2010). RNAi of *apl-1* rescues *let-7* mutant phenotypes of vulva bursting, extra molts, and lethality (Niwa *et al.* 2008), suggesting that *apl-1* is negatively regulated by *let-7* during the L4-to-adult transition. Although no *let-7* binding sites are present in the 3′-UTR of *apl-1*, other miRNA binding sites have been found in the 3′-UTR of *apl-1* (Figure 1) (Niwa *et al.* 2008).

The only viable *apl-1* mutant isolated thus far, *apl-1(yn5)*, contains a deletion mutation that removes the coding region for the transmembrane and cytoplasmic portions of the APL-1 protein and a large portion of the 3′-UTR and produces only the extracellular domain of APL-1, again demonstrating that the APL-1 extracellular domain is sufficient for viability (Figure 1) (Hornsten *et al.* 2007). *apl-1(yn5)* mutants show several phenotypes, including a slowed development compared to wild-type animals (Hornsten *et al.* 2007). In this study, we investigate the function of the extracellular domain of APL-1 during development. In addition to the slowed development, *apl-1(yn5)* mutants have several other phenotypes, including a temperature-sensitive embryonic lethality. We determined that several of the *apl-1(yn5)* phenotypes can be suppressed by *daf-16* FOXO and *daf-12* NHR mutations. Furthermore, we performed a small scale modifier screen to isolate enhancers and suppressors of the temperature-sensitive lethality of *apl-1(yn5)* mutants.

Materials and Methods

Strains

C. elegans strains were grown and maintained on MYOB plates (Church *et al.* 1995) containing OP50 *Escherichia coli* bacteria at 20° using methods as described (Brenner 1974), unless noted. All mutations used are described in WormBase (www.wormbase.org) and include: LGI: *daf-16(mu86)* (Lin *et al.* 1997); LGII: *moa-2/*B0495.6*(yn39)*; LGIII: *moa-1/*R155.2*(yn38)*, *daf-2(e1370)* (Kimura *et al.* 1997); LGIV: *flp-1(ok2781)*; and LGX: *daf-12(m20)* (Larsen *et al.* 1995), *apl-1(yn5* and *yn10)* (Hornsten *et al.* 2007). Construction of transgenes to rescue modifiers of the temperature-sensitive *apl-1(yn5)* lethality: phusion high-fidelity polymerase (Finnzymes) was used to amplify the genomic region, including the promoter and 3′-UTR, corresponding to genes of

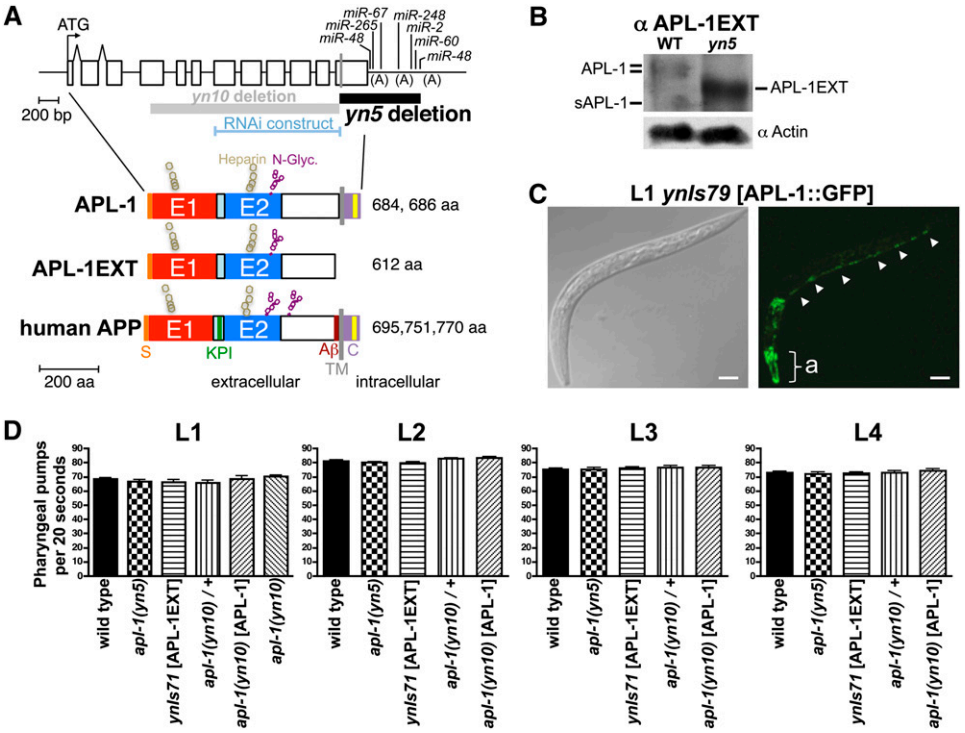

Figure 1 *apl-1(yn5)* mutants have increased levels of the APL-1 extracellular fragment. (A) Schematic of genomic organization of *apl-1* and corresponding APL-1 protein compared with human APP. The 3′-UTR of *apl-1* has three possible polyadenylation sites (A), all of which are used *in vivo* (Daigle and Li 1993), and several possible microRNA (miR) binding sites. The *yn5* allele deletes the region encoding the transmembrane domain (gray vertical line) and the entire cytoplasmic domain, and a large part of the 3′-UTR, including two of the three polyadenylation sites. S, signal peptide; KPI, Kunitz-type protease inhibitor sequence (not present in APP695 or APL-1); Aβ, amyloid peptide; the extracellular domain contains the conserved E1 and E2 domains, which share 46 and 49% similarity between *C. elegans* APL-1 and human APP695, respectively (Daigle and Li 1993). The E1 domain contains a putative growth-factor–like domain, copper, zinc and heparin binding domains, and 12 conserved cysteines followed by an acidic rich region (aqua box) (Daigle and Li 1993). The E2 domain contains an N-glycosylation site (N-Glyc) and heparin-binding domain. The crystal structure of the APL-1 E2 domain is similar to the human APP E2 domain (Hoopes *et al.* 2010). The cytoplasmic domain (indicated by C) shows 71% similarity between *C. elegans* APL-1 and human APP695, has a conserved YENPTY internalization signal (yellow), a consensus sequence for G_o binding, and four of the seven conserved phosphorylation sites of APP. (B) Western blot of mixed stage wild-type (WT) animals probed with an antibody against the extracellular domain of APL-1 (αAPL-1EXT) show proteins corresponding to glycosylated and unmodified full-length APL-1 (double bars) and one protein corresponding to the cleaved extracellular APL-1, sAPL-1. *apl-1(yn5)* mutants show high levels of APL-1EXT, which is slightly larger than sAPL-1. (C) Expression pattern of translational fusion of APL-1 protein with GFP (*ynIs79* [APL-1::GFP]) of first larval stage *C. elegans*. APL-1 is expressed in head neurons (lower left), arcade cells (a), and ventral cord neurons (arrowheads). Bar, 20 μm. (D) Pharyngeal pumping rates of heterozygous *apl-1(yn10)* null mutants, homozygous *apl-1(yn5)* mutants, or transgenic animals overexpressing full-length APL-1 (*apl-1(yn10)* [APL-1]) or the extracellular domain of APL-1 (*ynIs71* [APL-1EXT]) were similar to the pharyngeal pumping rate of wild-type animals during all four larval stages (L1–L4; N > 30 for each larval stage). Because complete loss of *apl-1* leads to a molting defect during the first to second larval stage transition, the pharyngeal pumping rate for homozygous *apl-1(yn10)* mutants could only be scored for the first larval stage (L1).

interest from wild-type (N2 var. Bristol) genomic DNA. The following primer pairs (5′ to 3′) were used: *tag-235*, Ptag235F (ggaacgagtgatgtgaggcag)/3tag235R (cggtgcctgttggagattcg); *dnj-24*, Pdnj24F3 (gccaaactctcggccaactc)/dnj24R (tacgtgcctcatggctctcc); *moa-1*/R155.2, P-R155-F1 (gctctggaaccggcttatgg)/3-R155-R1 (cgtaggccgcttccaaacaac); and *moa-2*/B0495.6, 3-operon-*Kpn*I (agagggtaccgaaaggacgtgcgggaaagc; restriction site underlined)/5-operon2 (gcggcaagggaatagtcagag) and 5-B0495-*Kpn*I (agagggtaccggagtacggtggacaagtacg; restriction site underlined)/B0495-3o (gagcattccacggttgtcgtc). The *moa-2*/B0495.6 products were digested with *Kpn*I and ligated together. Amplified fragments were gel purified and inserted into a TOPO Blunt vector (Invitrogen), which was used for microinjection into *yn38*; *apl-1(yn5)* or *yn39*; *apl-1(yn5)* animals. Extrachromosomal transgenic lines generated were (transgenes are indicated in brackets; unless otherwise noted, the promoter used was that of the indicated gene and the transgene contained a wild-type copy of the gene): *ynEx201* [*tag-235*; *sur-5*::GFP], *ynEx202* [*tag-235*; *sur-5*::GFP], *ynEx207* [*dnj-24*; *tag-235*; *sur-5*::GFP], *ynEx208* [*dnj-24*; *sur-5*::GFP], *ynEx203* [R155.2; *sur-5*::GFP], *ynEx204* [R155.2; *sur-5*::GFP], *ynEx205* [R155.2; *sur-5*::GFP], *ynEx206* [R155.2; *sur-5*::GFP], *ynEx209* [B0495.6; *sur-5*::GFP], *ynEx210* [B0495.6; *sur-5*::GFP], and *ynEx211* [B0495.6; *sur-5*::GFP]. Construction of the APL-1 transgenes and the resulting transgenic lines are described (Hornsten *et al.* 2007). Integrated *apl-1* transgenic lines used were (transgenes are indicated in brackets; unless otherwise noted, the promoter used was the *apl-1* promoter): *ynIs106* [*apl-1*(*yn32 yn5*), P*myo-2*::GFP]; LGIV: *zIs356* [*daf-16*::GFP, pRF4 *rol-6(su1006gf)*] (Henderson and Johnson 2001); LGV: *ynIs71* [*apl-1*(*yn5*), *sur-5*::GFP], *ynIs79* [*apl-1*::GFP], *ynIs100* [*apl-1*(*yn32*)::GFP, pRF4 *rol-6(su1006gf)*]; and LGX: *ynIs86* [*apl-1*, *sur-5*::GFP], and *ynIs107* [*apl-1*(*yn32*/D342C/S362C)::GFP, P*myo-2*::GFP] (Hoopes *et al.* 2010). For simplicity in the text, we will only indicate the protein expressed by the transgenes, including GFP-tagged proteins, in brackets; unless otherwise indicated, the *apl-1* promoter was used to express the transgene.

Western blot analysis

Preparations of animal lysates and Western blots were performed as described; protein levels were normalized to

levels of actin (Hornsten *et al.* 2007). Roughly the same extract amount for each strain was electrophoresed and transferred. After transferring, the blot was cut in two: one blot was probed with an antiserum against the extracellular domain of APL-1 (1:2000) (Hornsten *et al.* 2007) and one blot was probed with an actin monoclonal antibody (JLA20 at 1:500; Developmental Studies Hybridoma Bank); secondary antibodies were used at 1:4000 to 1:2000. Relative protein levels were determined by relative intensity to wild type (N2) using National Institutes of Health ImageJ Gel analyzer.

Pharyngeal pumping rate assays

To synchronize worm populations ~15 gravid adult worms were placed into a bleach solution to release the eggs. Hatched worms were raised at 20°. Developmental stage was measured by gonadal development. Pharyngeal pumping rate was measure by visually counting the movement of the pharyngeal grinder on a stereomicroscope for a period of 20 sec. Only worms on the bacterial food source and with constant pharyngeal pumping were scored.

Developmental timing and egg-laying rate assays

To synchronize worm populations ~15 gravid adult worms were placed into a bleach solution to release the eggs. Hatched worms were raised at 20°. Four days later [or 5 days for slower developing strains such as *apl-1(yn5)* and *zIs356*(DAF-16::GFP)], 10 synchronized adults were placed onto a fresh plate and allowed to lay eggs for 1–1.5 hr at room temperature (22–24°). Eggs were counted to determine an egg-laying rate; F_1 progeny were placed at 20° to allow development. After 70–72 hr, the developmental stages of the animals at 20° were scored according to their gonadal development and body size. For development at 25°, animals were scored after 48 hr. Each individual trial was performed with at least three plates of synchronized eggs for each strain and always included wild-type animals as a control. For statistical analysis for the egg-laying rate, one-way ANOVAs with Tukey's post-test (95% confidence intervals) were performed to assess similarity between groups and for developmental timing, a χ^2 test was performed using Prism 4.0a software (GraphPad).

Body length measurements

For each individual trial, 30 L4 animals (10 L4 per plate) for each strain were picked and allowed to develop for 3 days at room temperature (22–24°). Animals were mounted onto 2% agar pads containing a drop of 10 mM NaN_3 and pictures of the animals were taken at ×100 magnification on a confocal microscope (Zeiss LSM 510 confocal laser scanning system). The lengths of the worms were determined by drawing a line along the midline of the animals from the tip of the mouth to the tail. For statistical analysis one-way ANOVAs with Tukey's post-test (95% confidence intervals) were performed to assess similarity between groups using Prism 4.0a software (GraphPad).

Critical period assays

Ten synchronized gravid adults were placed onto a fresh plate and allowed to lay eggs for 0.5, 1, or a maximum of 1.5 hr at 15°. Eggs were counted and adult P_o were killed; F_1 progeny were either shifted to 27° or placed back at 15° to allow development, so that eggs in intervals of 30 min up to 6 hr were shifted to 27°. After 44 hr at 27°, the developmental stages and number of surviving animals were scored. Each individual trial was performed with at least three plates of synchronized eggs for each strain and always included wild type as a control. For statistical analysis one-way ANOVAs with Tukey's post-test (95% confidence intervals) were performed to assess similarity between groups using Prism 4.0a software (GraphPad).

RNA interference assays

RNAi by feeding: day −1, a single RNAi clone [HT115 bacteria, which are maintained at −80° on Luria broth medium (LB) agar plates with 25 μg/ml carbenicillin and 12.5 μg/ml tetracycline] was picked from the Ahringer library (Kamath *et al.* 2001) (Geneservice) and incubated in 1 ml LB containing 100 μg/ml ampicillin (at 37°, 280 rpm) overnight; day 0, the 1-ml bacterial culture was transferred into 10 ml LB containing 100 μg/ml ampicillin and incubated for another 4–6 hr at 37° at 280 rpm. A total of 450 μl of the bacteria culture was spread onto MYOB plates (Church *et al.* 1995) containing 400 mM of βD-isothiogalactopyranoside (IPTG) and 50 μg/ml ampicillin, and these RNAi plates were placed in 37° overnight; day 1, eight L4 animals (P_o) were placed on bacteria lawn that express double-stranded RNA (dsRNA) of target gene or empty vector control (L4440) to knock down expression levels of the targeted gene; day 4, ~50 F_1 L4 animals were transferred onto new plates containing the same dsRNA-expressing bacteria; day 5, ~10 F_1 1-day-old adults were transferred onto new plates containing the same dsRNA-expressing bacteria to lay eggs for 1–1.5 hr at 20°; F_2 eggs were placed at either 20° or 27°; and day 8, the F_2 population was scored for developmental progression and survival.

DAF-16::GFP nuclear translocation assays

L4 animals were placed onto new plates and grown at 20°. One day later, animals were placed at 35° and scored at different times (T = 0, 30, 60, 90, 120, and 150 min) by mounting the animals onto 2% agar pads containing a drop of M9 physiological buffer (Brenner 1974) and looking at the worms at ×100 magnification on a Zeiss Axioplan microscope. To ensure exact timing, the individual strains were placed at 35° in 5-min intervals. Upon 35° heat stress, DAF-16::GFP translocates from the cytoplasm into the nucleus (Henderson and Johnson 2001). The rate of DAF-16::GFP nuclear translocation was scored as described (Curran and Ruvkun 2007): category 0: all DAF-16::GFP showing diffuse localization in the cytoplasm; category 1: more DAF-16::GFP localized in cytoplasm than in nucleus; category 2: more

DAF-16::GFP localized in nucleus than in cytoplasm; category 3: almost all DAF-16::GFP localized in nucleus. Statistical significance was determined by a χ^2 test using Prism 4.0a software (GraphPad).

Mutagenesis screen and mapping

Worms were mutagenized with 50 mM EMS as described (Brenner 1974). Mutagenized L4 animals (P_o) were singly plated and placed at 20° to develop until F_1 animals reached adulthood. Ten F_1 adults were allowed to lay F_2 eggs, which were then shifted to 27°. Plates on which the number of F_2 progeny was greater or smaller than the number of progeny from nonmutagenized *apl-1(yn5)* mutants were selected for further analysis. A total of 200 haploid genomes were screened and five mutants were isolated. The strongest suppressor (*yn38*) and enhancer (*yn39*) of the *apl-1(yn5)* lethality at 27° were selected for further characterization. *yn38* was mapped by conventional methods (Brenner 1974) to chromosome III and *yn39* was mapped using SNPs to chromosome II as described (Davis *et al.* 2005). The DNA from both mutants was isolated and used for whole genome deep sequencing as described (Sarin *et al.* 2010).

Results

Expression of the extracellular domain of APL-1 is sufficient to slow developmental progression

Wild-type *C. elegans* have a very stereotyped pattern of cell divisions. Synchronized eggs develop into fourth stage (L4) larva within 65 hr and into adults by 72 hr at 20° (Ailion and Thomas 2000). By contrast, *apl-1(yn5)* mutants were found mostly in L4 or earlier larval stages at 72 hr (Figure 2; Table 1) (Hornsten *et al.* 2007). As predicted from the mutation (Figure 1), *apl-1(yn5)* mutants contained high levels of only the extracellular fragment of APL-1 (APL-1EXT), which is slightly larger than the cleaved sAPL-1 produced in wild-type animals (Figure 1) (Hornsten *et al.* 2007). The slowed developmental progression of *apl-1(yn5)* mutants can be phenocopied in wild-type animals by microinjection of an APL-1EXT fragment (*ynIs71*) (Table 1). As a control, we generated an APL-1EXT transgene that contained a mutation corresponding to the *apl-1*(*yn32*) null mutation [APL-1EXT (*yn32*)]; transgenic animals carrying this transgene (*ynIs106*) did not rescue *apl-1* knockouts and these transgenic animals developed at the same rate as wild-type animals (Table 1). These results indicate that overexpression of APL-1EXT and presumably sAPL-1 is sufficient to slow developmental progression.

Although the *apl-1(yn5)* mutation appears to delay developmental progression by one larval stage (Table 1), in actuality the delay is more significant. After fertilization, wild-type eggs develop and are laid when they reach about the 30-cell stage of division (Sulston *et al.* 1983). *apl-1(yn5)* mutants retain eggs in the uterus longer than wild-type animals; eggs laid by *apl-1(yn5)* mutants, therefore, are chronologically older than eggs laid by wild-type animals. For instance, at 15° most wild-type eggs were at the 30- to 100-cell stage after 30 min or at the comma stage after 6 hr after being laid. By contrast, most *apl-1(yn5)* eggs were already in the comma stage after 30 min or the threefold (pretzel) stage 6 hr after being laid at 15°; the time to progress from the comma stage to the pretzel stage is about half the time to progress from the 30- to 100-cell stage to the comma stage (see Figure 4 below). Hence, the *apl-1(yn5)* mutation causes a severe delay in developmental progression.

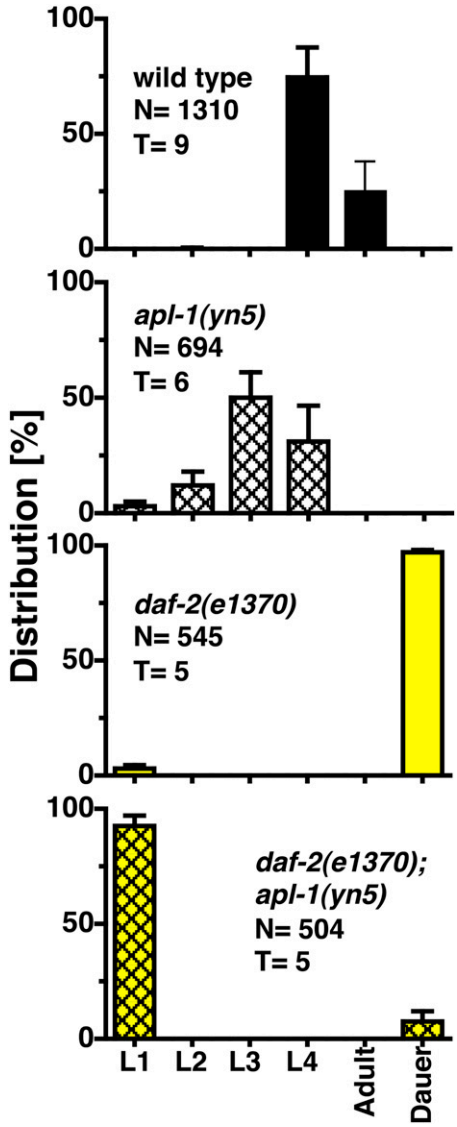

Figure 2 *apl-1(yn5)* mutants show a slowed developmental progression that is enhanced by decreased *daf-2* activity. After 48 hr at 25°, all eggs from wild-type animals developed into L4 or adult animals. By contrast, *apl-1(yn5)* mutants developed mostly into L3 or L4 animals and *daf-2 (e1370)* mutants mainly transitioned into an alternative dauer stage. Most *daf-2(e1370); apl-1(yn5)* double mutants, however, arrest in the L1 stage at 25°. *N* = number of animals, *T* = number of independent trials. Table 1 shows detailed statistical analysis and results of additional strains.

One possible explanation for the slowed development of *apl-1(yn5)* animals could be a lower feeding rate of the animals, thereby leading to a slower metabolic rate and

Table 1 The delayed development of *apl-1(yn5)* mutants requires *daf-12* and *daf-16* activity

Strain (genotype)	N_{eggs}	L1 (%)	L2 (%)	L3 (%)	L4 (%)	Adult (%)	N_{worms} (*T*)	Average survival 20° (%) ± STE	N_{eggs} (*T*)	L1 (%)	L2 (%)	L3 (%)	L4 (%)	Adult (%)	Dauer (%)	Average survival 25° (%) ± STE
Wild type (N2)	3462	0	0	0	3	97	3572 (30)	103 ± 0.7	1310 (9)	0	0	0	75	25	0	104 ± 3.0
ynIs106 [APL-1EXT(*yn32*)]	256	0	0	0	0	100	259 (3)	98 ± 10.7	349 (3)	0	0	0	94	6	0	100 ± 1.1
apl-1(yn5)	943	1	2	10	82	5	826 (11)[a]	86 ± 1.7[a]	694 (6)[a]	4	13	51	32	0	0	75 ± 2.1[a]
ynIs71 [APL-1EXT]	488	1	1	2	37	59	397 (6)[a]	82 ± 4.5[a]	283 (3)[a]	9	29	60	2	0	0	64 ± 8.6[a]
daf-12(m20)	936	0	0	0	1	99	921 (7)	97 ± 7.3	581 (5)[a]	20	66	10	4	0	0	90 ± 4.5
daf-12(m20); ynIs71	244	0	0	0	7	93	197 (3)	80 ± 6.2[a,b]	253 (5)[a]	24	65	6	5	0	0	75 ± 3.7[a,b]
N2 grown on L4440 RNAi	320	0	0	0	0	100	323 (3)	99 ± 1.5								
N2 grown on *daf-12* RNAi	766	0	0	0	0	100	733 (3)	95 ± 3.1								
daf-12(m20) grown on L4440 RNAi	366	0	0	0	0	100	332 (3)	91 ± 5.4								
daf-12(m20) grown on *daf-12* RNAi	460	0	0	0	0	100	404 (3)	89 ± 5.9								
apl-1(yn5) grown on L4440 RNAi	683	1	0	4	95	0	538 (3)[a]	78 ± 4.8[c]								
apl-1(yn5) grown on *daf-12* RNAi	743	0	0	0	0	100	608 (3)	81 ± 6.5[c]								
daf-16(mu86)	579	0	0	0	1	99	597 (5)	100 ± 1.6	953 (11)	1	2	5	92	0	0	98 ± 1.9
daf-16(mu86); apl-1(yn5)	1272	8	5	3	11	73	1115 (4)[d]	85 ± 7.0[a,e]	838 (8)[d]	5	2	14	79	0	0	36 ± 4.3[a,d]
zIs356 [DAF-16::GFP]	2241	0	1	9	90	0	2236 (12)[a]	99 ± 1.8	468 (5)[a]	7	0	0	0	0	93	81 ± 3.8[a]
zIs356 [DAF-16::GFP]; *apl-1(yn5)*	1165	1	26	60	13	0	1031 (3)[a,d,f]	90 ± 4.9[a]	781 (7)[a,d,f]	73	24	0	0	0	3	79 ± 4.6[a]
daf-2(e1370)[g]	748	1	0	2	93	1	691 (4)[a]	92 ± 7.7	545 (5)[a]	3	0	0	0	0	97	89 ± 5.2
daf-2(e1370); apl-1(yn5)[h]	416	10	13	77	0	0	283 (3)[a,i]	69 ± 11.2[a,d,i]	504 (5)[a,d,i]	92	0	0	0	0	8	42 ± 5.2[a,d,i]
daf-2(e1370); daf-16(mu86)[h]	299	0	1	1	3	95	271 (3)[i]	91 ± 5.7	354 (3)[i]	2	1	4	93	0	0	83 ± 2.5[a,e]
daf-2(e1370); daf-16(mu86); apl-1(yn5)[h]	371	6	8	2	19	65	254 (3)[d,i]	68 ± 8.9[a,d,e,i]	209 (3)[d,i]	17	2	8	73	0	0	47 ± 14.6[a,d,e,i]

Developmental stage of animals was scored 72 and 48 hr after eggs were laid at 20° and 25°, respectively. All developmental distributions are shown in cumulative form. *Is* alleles indicate integrated transgenes. Transgenes shown in brackets. Transgenes were driven by the *apl-1* promoter unless otherwise noted; the encoded protein is indicated; DAF-16::GFP is driven by the *daf-16* promoter. *ynIs106* carries a transgene that contains the *apl-1(yn32)* missense mutation in the region encoding the extracellular domain; this transgene does not rescue *apl-1(yn10)* null lethality and is considered a nonfunctional APL-1EXT control. *N* = number of animals observed. *T* = number of independent times experiment was performed. L4440 RNAi, empty vector control. Note that Gems *et al.* (1998) reported that *daf-2(e1370); daf-12(m20)* animals at 25.5° were found as L1 (43%) and L2 or L3 (57%), but no dauers or adults were observed. SUR-5::GFP was used as a co-injection marker for *ynIs71* and *ynIs86*, P*myo-2*::GFP for *ynIs106*, and *rol-6(su1006)* for *ynIs79* and ynIs100. For statistical analysis: *P*-values were determined by one-way ANOVAs with Tukey post-test (95% confidence intervals) for survival rate and χ^2 (4 d.f.) for developmental progression and are only indicated when $P < 0.001$. For *P*-values against controls at the indicated temperature, see footnotes [a–f] and [i]. STE, standard error.

[a] wild type
[b] *daf-12(m20)*
[c] wild type on RNAi L4440
[d] *apl-1(yn5)*
[e] *daf-16(mu86)*
[f] *zIs356* [DAF-16::GFP]
[g] form on average 3% dauers
[h] no dauers observed at 20°
[i] *daf-2(e1370)*

developmental delay. We tested whether modulating *apl-1* levels affected feeding by measuring pharyngeal pumping rates. Heterozygous *apl-1(yn10)* animals, which carry an *apl-1(yn10)* null allele, homozygous *apl-1(yn5)* mutants, or transgenic animals carrying the APL-1EXT transgene showed pumping rates similar to wild-type animals during all four larval stages (L1–L4; Figure 1D). Because homozygous *apl-1(yn10)* mutants die during the L1-to-L2 transition (Hornsten *et al.* 2007; Wiese *et al.* 2010), we were only able to measure the pumping rates of homozygous *apl-1(yn10)* animals during L1; the homozygous *apl-1(yn10)* L1 animals also had pumping rates similar to wild type (Figure 1D). These results suggest that neither overexpression of APL-1EXT nor decreased *apl-1* activity have any affect on feeding rates during development. These results are in contrast to the increased pharyngeal pumping rates when *apl-1* was knocked down by RNAi through microinjection (Zambrano *et al.* 2002).

apl-1(yn5) enhances daf-2-induced L1 arrest but not dauer formation

Different environmental conditions result in the activation of multiple parallel pathways that determine the animal's developmental progression and adjust the animal's metabolic processes accordingly (reviewed in Fielenbach and Antebi 2008). *apl-1(yn5)* mutants could show a slowed development because of altered metabolic processes. We examined the effects of altering the insulin signaling pathway, a key metabolic pathway in *C. elegans* as well as mammals, in *apl-1(yn5)* mutants.

Activation of the insulin pathway is necessary for reproductive growth (Gems *et al.* 1998), whereas unfavorable environmental conditions lead to decreased insulin signaling in *C. elegans* (Henderson and Johnson 2001). Even in the presence of food, strongly reducing *daf-2* insulin/IGF-1 receptor activity induces L1 arrest (Gems *et al.* 1998; Baugh and Sternberg 2006), while slightly reducing *daf-2* activity induces dauer formation (Kimura *et al.* 1997). The L1 arrest due to decreased *daf-2* activity requires the activity of *daf-16* FOXO (Table 1; Baugh and Sternberg 2006). Animals with a weak temperature-sensitive *daf-2(e1370)* mutation have a slowed progression through all larval stages at the 20° permissive temperature (Table 1); in addition, ~3% of the animals (23 dauers/748 total) enter the dauer stage compared to none of the wild-type animals (0 dauers/3572 total) or *apl-1(yn5)* mutants (0 dauers/943 total). At the nonpermissive temperature of 25°, all wild-type animals developed into L4 or adult animals after 48 hr (Figure 1) (Kimura *et al.* 1997; Gems *et al.* 1998), whereas 97% (528/545 total) of *daf-2(e1370)* mutants enter the dauer stage and 3% enter L1 arrest (Figure 2; Table 1) (Kimura *et al.* 1997; Gems *et al.* 1998).

To determine whether *apl-1* signaling modulates the insulin signaling pathway, we examined *daf-2(e1370)*; *apl-1(yn5)* double mutants. *daf-2(e1370)*; *apl-1(yn5)* double mutants showed an even slower developmental progression at 20° than *daf-2(e1370)* or *apl-1(yn5)* single mutants, but the rate of dauer formation was not increased (Table 1). Furthermore, the percentage of *daf-2(e1370)*; *apl-1(yn5)* double mutants entering L1 arrest at 25° was greatly enhanced: 92% of *daf-2(e1370)*; *apl-1(yn5)* double mutants entered L1 arrest, while the remaining 8% became dauer animals (Figure 2; Table 1). Thus, *apl-1(yn5)* activity either reduces the activity of the insulin/IGF-1 signaling pathway or acts in parallel to the insulin pathway to enhance L1 arrest and delay development.

The slowed development of apl-1(yn5) mutants requires the activity of daf-16 and daf-12

Signaling through the *daf-2* insulin/IGF-1 receptor decreases *daf-16* activity. *daf-16(mu86)* mutants showed a similar developmental progression pattern as wild-type animals, whereas overexpression of *daf-16* with a functional translational fusion of DAF-16 with green fluorescent protein (DAF-16::GFP) slows developmental progression, such that most animals are in the L4 stage after 72 hr (Table 1) (Henderson and Johnson 2001). To determine whether the development of *apl-1(yn5)* mutants is affected by *daf-16* activity, we made *daf-16(mu86)*; *apl-1(yn5)* double mutants. *daf-16(mu86)*; *apl-1(yn5)* double mutants showed a similar developmental progression as *daf-16(mu86)* or wild-type animals (Table 1), indicating that the slowed development of *apl-1(yn5)* mutants requires *daf-16* activity. Moreover, the increased rate of L1 arrest in *daf-2(e1370)*; *apl-1(yn5)* double mutants was suppressed by loss of *daf-16* activity (Table 1). At 25°, 73% of the *daf-2(e1370)*; *daf-16(mu86)*; *apl-1(yn5)* triple mutants developed into L4 (73% in L4; 8% in L3, 2% in L2, and 17% in L1; Table 1). By contrast, the *apl-1(yn5)* mutation was additive to the effects of DAF-16 overexpression: after 72 hr DAF-16::GFP; *apl-1(yn5)* animals are mostly found in the L2–L3 stage. These results suggest that APL-1EXT, and presumably sAPL-1, signal to modulate the insulin pathway, thereby increasing *daf-16* activity to affect developmental progression.

The insulin pathway converges with a parallel pathway that signals through the DAF-12 nuclear hormone receptor (NHR) during the developmental decision to enter reproductive growth or dauer formation. While L1 arrest requires *daf-16* activity (Baugh and Sternberg 2006), dauer formation (Lin *et al.* 1997; Ogg *et al.* 1997) is regulated by DAF-12 NHR as well as DAF-16 FOXO activity (Henderson and Johnson 2001; Lee *et al.* 2001; Lin *et al.* 2001). *daf-12* NHR and *daf-16* FOXO are expressed ubiquitously (Antebi *et al.* 2000; Henderson and Johnson 2001; Lee *et al.* 2001; Lin *et al.* 2001) and *daf-12(m20)* and *daf-16(mu86)* null mutants are dauer defective (Vowels and Thomas 1992; Larsen *et al.* 1995; Antebi *et al.* 2000). In addition, *daf-12* NHR also plays an important role in developmental timing by forming a feedback loop with the *let-7* miRNA family of heterochronic genes (Hammell *et al.* 2009) and by acting in a complex genetic network with the *lin-42* period gene (Monsalve *et al.* 2011).

To determine whether *daf-12* activity is necessary for the slowed development in *apl-1(yn5)* mutants, we knocked down *daf-12* activity in *apl-1(yn5)* mutants by RNAi. The slowed development of *apl-1(yn5)* mutants was suppressed by *daf-12* NHR knockdown, whereas *daf-12* RNAi had no effect on developmental progression of wild-type or *daf-12 (m20)* mutant animals (Table 1). Similarly, the slowed development of *ynIs71* [APL-1EXT] overexpression animals was rescued in a *daf-12(m20)* mutant background (Table 1), excluding an RNAi off-target effect of *daf-12* RNAi. Signaling of the extracellular domain of APL-1, therefore, requires DAF-12 NHR activity to delay development.

apl-1(yn5) slows DAF-16 nuclear localization under heat-shock conditions

Because APL-1EXT is a released fragment, APL-1EXT signaling will influence DAF-16 activity indirectly. Since *C. elegans* is transparent, DAF-16 localization can be monitored by using DAF-16::GFP. Under well-fed, noncrowded, and unstressed laboratory conditions, DAF-16::GFP is predominantly found diffused in the cytoplasm of all cells in wild-type (Henderson and Johnson 2001) and *apl-1(yn5)* animals (Supporting Information, Table S1). Translocation of DAF-16::GFP from the cytoplasm to the nucleus can be visualized in intestinal cells by putting animals under a heat stress (Henderson and Johnson 2001). When DAF-16::GFP animals were shifted from 20° to 35°, DAF-16::GFP translocated into the nucleus within 3 hr (Table S1) (Henderson and Johnson 2001). DAF-16::GFP; *apl-1(yn5)* animals showed a delayed DAF-16::GFP nuclear translocation compared to DAF-16::GFP animals at 35° (Table S1). As a control, nonfunctional APL-1EXT [APL-1EXT*(yn32)*] did not alter the timing of DAF-16::GFP nuclear translocation (DAF-16::GFP; *ynIs106*; Table S1). These results indicate that APL-1EXT activity slows intestinal DAF-16 nuclear translocation in response to stress. Thus, *apl-1* acts in multiple pathways to affect DAF-16 FOXO activity.

Several apl-1(yn5)–induced phenotypes require daf-16 FOXO and daf-12 NHR activity

Our results suggest that *apl-1(yn5)* acts in multiple pathways that converge on *daf-16* FOXO and *daf-12* NHR. Alterations in the TGFβ signaling pathway can lead to DAF-16 nuclear localization (Lee *et al.* 2001; Shaw *et al.* 2007; Jeong *et al.* 2010) and there is an extensive cross-talk between the insulin/IGF-1 and TGFβ pathways for multiple processes (Narasimhan *et al.* 2011). Consequently, we examined whether *daf-16* FOXO and *daf-12* NHR activity mediate other *apl-1(yn5)* phenotypes. Body size in *C. elegans* is regulated by genetic and environmental factors through the insulin (So *et al.* 2011) and TGFβ pathways (Savage-Dunn *et al.* 2003). Wild-type adult animals are 1225 ± 6.6 μm (n = 172) in length. *apl-1(yn5)* mutants and transgenic animals carrying an APL-1EXT transgene (*ynIs71*) were 15% (1047 ± 11.6 μm, n = 63) or 27% (894 ± 28.2 μm, n = 33) shorter, respectively, than wild-type animals (Figure 2A; Table S2), indicating that the shortened body length is due to high levels of APL-1EXT and not due to loss of the APL-1 intracellular domain (*C. elegans* AICD). Similarly, animals that overexpress full-length APL-1 (*ynIs86* and *ynIs79*) were 12–20% shorter than wild-type animals, whereas animals that carry a transgene with a mutated *apl-1* (*ynIs100*) were wild type in length (Figure 3A; Table S2). Thus, *apl-1* activity, and specifically the activity of sAPL-1, affects body length.

daf-2(e1370) mutants are also slightly shorter than wild type (Figure 3A). The shortened body length of *apl-1(yn5)* mutants was enhanced when *daf-2* activity was decreased (Figure 3A), suggesting that, as with developmental progression, *apl-1(yn5)* activity either reduces the activity of the insulin/IGF-1 signaling pathway or acts in parallel to the insulin pathway to affect body size. *daf-16(mu86)* mutants were slightly (3%) longer and DAF-16::GFP animals were slightly shorter than wild type, although both not significantly; similarly, *daf-12(m20)* mutants were similar in length to wild-type animals (Figure 3A; Table S2). In a *daf-16(mu86)* background, *apl-1(yn5)* mutants and transgenic APL-1 overexpression lines were the same length as *daf-16(mu86)* mutants (Figure 3A; Table S2), suggesting that the shorter body length of *apl-1(yn5)* mutants requires *daf-16* activity. Moreover, the shortened body size of the *daf-2(e1370)*; *apl-1(yn5)* double mutants was rescued to wild-type length in a *daf-16(mu86)* background (Figure 3A). Similarly, in a *daf-12(m20)* background, transgenic APL-1 overexpression lines were the same length as *daf-12(m20)* mutants (Figure 3A; Table S2). Furthermore, RNAi knockdown of *daf-12* in *apl-1(yn5)* mutants was sufficient to rescue the *apl-1(yn5)* shortened body length (Table S2). Hence, both *daf-16* FOXO and *daf-12* NHR activity are required for the shortened body length of *apl-1(yn5)* animals. By contrast, DAF-16 overexpression enhanced the shortened body length of transgenic APL-1 overexpression lines (Table S2). Collectively, these results suggest that *apl-1* activity modulates the insulin pathway to increase *daf-16* activity to affect body size.

APL-1 is expressed in vulval hypodermal cells and vulval muscles cells, which regulate egg laying (Hornsten *et al.* 2007). *apl-1(yn5)* mutants, as well as transgenic APL-1 or APL-1EXT overexpression lines (data not shown), retain eggs and show a decreased egg-laying rate (Hornsten *et al.* 2007), suggesting that this phenotype is due to high levels of APL-1EXT and not due to loss of signaling through the *C. elegans* AICD fragment. Wild-type animals lay about seven eggs per hour, whereas *apl-1(yn5)* mutants lay about four eggs per hour (Figure 3B; Table S3) (Hornsten *et al.* 2007). Transgenic animals overexpressing either full-length APL-1 (*ynIs86* and *ynIs79*) or APL-1EXT (*ynIs71*) laid about five eggs an hour (Figure 3B; Table S3) (Hornsten *et al.* 2007). *daf-16(mu86)* mutants laid significantly more eggs, about nine eggs per hour, than wild-type animals (Figure 3B; Table S3). Transgenic APL-1 overexpression lines and *apl-1(yn5)* mutants carrying the *daf-16(mu86)* mutation laid eggs at

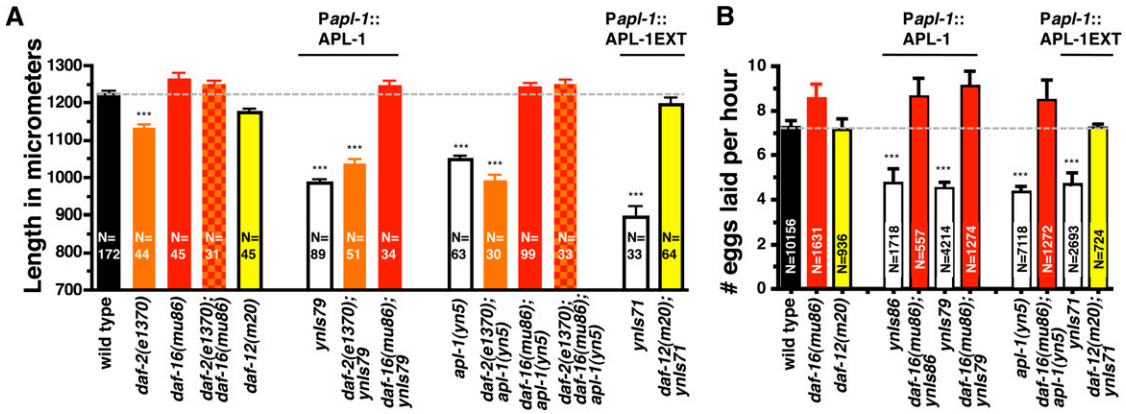

Figure 3 Decreased DAF-16 FOXO and DAF-12 NHR activity are required for APL-1 signaling to modulate body size and egg-laying rate. (A) Overexpression of APL-1 or APL-1EXT shortened the body length of the animal (white bars) compared to wild type (black bar). This shortened body length of *apl-1(yn5)* mutants and *ynIs79* [APL-1::GFP] transgenic animals was abolished in a *daf-16* null background and *ynIs71* [APL-1EXT] transgenic animals in a *daf-12(m20)* mutant background. Decreased *daf-2* activity enhances the shortened body length of *apl-1(yn5)* mutants. (B) Overexpression of APL-1 or APL-1EXT caused a reduction in the egg-laying rate (white bars); an egg-laying rate higher than wild type was restored in a *daf-16* null background or in a *daf-12(m20)* mutant background. Table S2 and Table S3 show detailed statistical analyses. Protein expressed by transgene in the transgenic lines (the *ynIs* strains) is indicated above the corresponding bars; *daf-16* null background is indicated in red, *daf-12(m20)* mutant background in yellow, and *daf-2 (e1370)* mutant background in orange; *Is*, integrated transgene. ***$P < 0.001$ determined by one-way ANOVA with Tukey's post-test.

the same rate as *daf-16(mu86)* mutants (Figure 3B; Table S3), suggesting that the egg-laying defect requires *daf-16* activity. Conversely, animals that overexpress DAF-16 showed a dramatic decrease in their egg-laying rate to about one to two eggs per hour (Table S3). Overexpression of full-length APL-1 (*ynIs79*) or the *apl-1(yn5)* mutation had no effect on the decreased egg-laying rate of DAF-16 overexpression animals (Table S3). *daf-12(m20)* mutants showed a similar egg-laying rate as wild-type animals (Figure 3B; Table S3). The decreased egg-laying rate of APL-1EXT overexpression animals (*ynIs71*) was completely rescued in a *daf-12(m20)* mutant background (Figure 3B; Table S3). These results suggest that APL-1EXT requires *daf-16* FOXO and *daf-12* NHR activity to decrease body length and egg-laying rate.

apl-1(yn5) mutants show a temperature-sensitive lethality and developmental arrest

As discussed above, at 20° and 25° wild-type animals hatch and develop into adults. At 27°, however, although all wild-type eggs hatch and animals survive (Table 2) (Ailion and Thomas 2000), ~10% of developing animals enter the dauer life cycle (Ailion and Thomas 2000). At 20°, 86% of the *apl-1(yn5)* mutants survived and 14% remained either arrested in L1 or died (Table 2). This lethality was enhanced at slightly higher temperatures: 75 and 47% of the *apl-1 (yn5)* mutants survived at 25° and 27°, respectively (Table 2). In addition, among the *apl-1(yn5)* mutants that survived, only a few developed into gravid adults and 46% remained in L1 arrest compared to only 1% of wild-type animals after 44 hr at 27° (Table 2); most of these *apl-1(yn5)* L1-arrested animals died within 5 days and showed morphological defects such that organs appeared detached from their underlying basal lamina and animals contained multiple vacuolar-like structures (data not shown). Thus, the *apl-1(yn5)* mutation causes a temperature-sensitive lethality and developmental progression block. To determine whether this lethality could be phenocopied, we examined transgenic APL-1EXT animals (*ynIs71*). A total of 82% of *ynIs71* [APL-1EXT] animals survived at 20°, 64% at 25°, and 54% at 27° (Table 2). Animals carrying the mutated APL-1EXT transgene [APL-1EXT*(yn32)*] (*ynIs106*) survived at similar rates to wild-type animals at 20° and 27° (Table 2). Hence, high levels of APL-1EXT, and presumably sAPL-1 activity is sufficient to cause a temperature-sensitive lethality and L1 arrest.

The critical period for the temperature-sensitive apl-1 (yn5) lethality is during embryogenesis

Because *apl-1(yn5)* mutants characteristically die after L1 arrest at 27°, we determined the critical time period of this temperature-sensitive lethality. Wild-type animals and *apl-1 (yn5)* mutants were allowed to lay eggs at 15°. Eggs were shifted to 27° at 30-min intervals and scored for survival 44 hr later. All wild-type eggs hatched and all animals survived from the different times (Figure 4). By contrast, the fraction of *apl-1(yn5)* eggs that hatched and survived increased linearly. At 30 min, 30% of *apl-1(yn5)* mutants survived, whereas shifting the eggs to 27° at 6 hr resulted in ~100% survival (Figure 4), indicating a critical time window of the *apl-1(yn5)*-induced lethality during embryogenesis. Specifically, *apl-1(yn5)* eggs that developed past the threefold (pretzel) embryonic stage at 15° survived the 27° shift (Figure 4), suggesting that the critical time period for APL-1 overexpression lethality is before the pretzel stage of embryonic development. These results would predict that all L1 APL-1 overexpression animals shifted to 27° should

Table 2 APL-1 overexpression causes a temperature-sensitive lethality

Strain (genotype)	20°					25°					27°				
	N_{eggs}	N_{worms}	T	Average % survival STE	% L1	N_{eggs}	N_{worms}	T	Average % survival STE	% L1	N_{eggs}	N_{worms}	T	Average % survival STE	% L1
Wild type (N2)	3462	3572	30	103 ± 0.7	0	1310	1351	9	104 ± 3.0	0	5633	6006	50	106 ± 1.6	1
ynIs107 [APL-1(*yn32*)D342C/S362C::GFP]	518	528	4	102 ± 1.4	0						810	816	8	100 ± 1.9	1
ynIs100 [*apl-1*(*yn32*)::GFP]	386	394	4	102 ± 2.3	0						575	621	6	106 ± 2.3	1
ynIs106 [*apl-1*(*yn5 yn32*)]	256	259	3	98 ± 10.7	0	349	352	3	101 ± 1.1	0	316	311	3	98 ± 1.4	0
ynIs86 [APL-1]	455	404	5	88 ± 4.5 *	0	420	315	4	77 ± 4.7 *	0	449	265	4	60 ± 3.5 *	31
ynIs79 [APL-1::GFP]	1015	639	10	63 ± 5.6 *	1	494	266	5	34 ± 10.8 *	3	1690	64	14	4.3 ± 0.9 *	47
ynIs71 [APL-1EXT]	488	397	6	82 ± 4.5 *	1	283	180	3	64 ± 8.6 *	9	484	261	5	54 ± 2.9 *	72
apl-1(yn5)	943	826	11	86 ± 1.7 *	2	694	512	6	75 ± 2.1 *	4	3737	1841	41	47 ± 1.9 *	46
apl-1(yn5); yn38	668	635	5	95 ± 4.8	2						497	480	5	96 ± 1.4 **	23
apl-1(yn5); yn39	364	237	3	69 ± 10.9 *,**	8						586	117	5	18 ± 2.9 *,**	69

ls alleles indicate integrated transgenes. Transgenes shown in brackets. Transgenes were driven by the *apl-1* promoter unless otherwise noted; the encoded protein is indicated; DAF-16::GFP is driven by the *daf-16* promoter. *apl-1(yn32)* is a missense mutation that corresponds to a null allele. N = number of animals observed. T = number of independent times or trials experiment was performed. SUR-5::GFP was used as a co-injection marker for *ynIs71* and *ynIs86*, *Pmyo-2*::GFP for *ynIs106* and *ynIs107*, and *rol-6(su1006)* for *ynIs79* and *ynIs100*. For statistical analysis: P-values were determined by one-way ANOVAs with Tukey post-test (95% confidence intervals) for survival rate and are only indicated if $P < 0.001$ against wild type (*) or *apl-1(yn5)* (**) at the given temperature. STE, standard error.

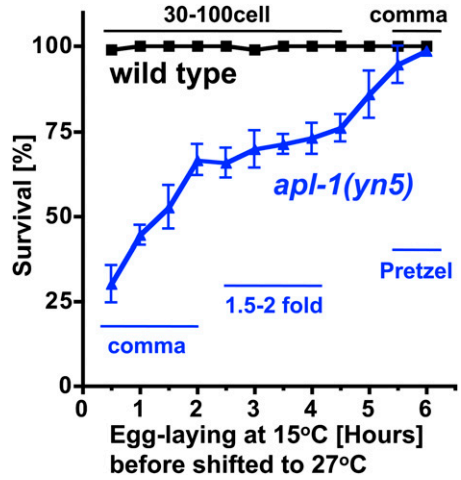

Figure 4 The critical time period for the *apl-1(yn5)* lethality is during embryogenesis. Eggs were laid at 15° and shifted at intervals of 30 min to 27°; plotted is the survival rate of those eggs after 44 hr at 27°. All wild-type eggs survive the 27° shift, whereas after shifting at 30 min, only 30% of the *apl-1(yn5)* eggs survived into larval stages. However, by letting the *apl-1(yn5)* eggs develop at 15° for 6 hr, all eggs survived and developed into larval animals. The developmental stage of eggs (30–100 cell, comma, 1.5- to 2-fold embryo, 3-fold embryo, pretzel) was scored at various time points. *apl-1(yn5)* eggs were chronologically further developed when laid compared to wild type, because *apl-1(yn5)* animals retained eggs longer in the uterus than wild-type animals. At least three trials for each time point ($N > 300$).

survive. Indeed, all *apl-1(yn5)* L1 mutants shifted to 27° survived ($N = 562$, $T = 5$), again restricting the APL-1–induced lethality to embryogenesis.

Knockdown of apl-1 by RNAi on apl-1(yn5) mutants causes a molting defect and lethality

Since *apl-1(yn5)* mutants have high levels of APL-1EXT (Figure 1) (Hornsten *et al.* 2007), we hypothesized that *apl-1* knockdown by RNAi could rescue the *apl-1(yn5)*-induced lethality. Surprisingly, feeding double stranded *apl-1* RNA to L4 *apl-1(yn5)* mutants resulted in dead L1–L4 animals in the next generation (F_1). These F_1 animals showed severe molting defects, similar to those seen in *apl-1 (yn10)* mutants, which show 100% lethality due to a molting defect during the first to second larval (L1/L2) stage transition. However, the RNAi *apl-1*–induced molting defect of *apl-1(yn5)* mutants occurred through all larval stages ($N > 30$ for each molting stage; 6 trials), suggesting that *apl-1* is required for molting not only during the L1/L2 transition, but during all larval transitions. We speculate that feeding *apl-1* RNAi to *apl-1(yn5)* mutants more efficiently knocks down *apl-1*, presumably because the *yn5* mRNA is smaller than wild type. Consistent with our observation that *apl-1* is needed for the molt in each larval transition, feeding RNAi of *apl-1* to worms in an RNAi-sensitized background [*rrf-3(pk1426)*] resulted in molting defects during L3/L4 and L4/adult transitions (Wiese *et al.* 2010).

Identification of suppressors and enhancers of the apl-1 (yn5) temperature-sensitive lethality

To identify genes in the pathway of *apl-1*, we performed a forward genetic screen for modifiers of the temperature-sensitive lethality of *apl-1(yn5)* mutants (Figure 5; Table 2). Mutagenized L4 animals were singly plated and 10 F_1 adults were allowed to lay F_2 eggs, which were then shifted to 27°. Plates on which the number of F_2 progeny was greater or smaller than the number of progeny from nonmutagenized *apl-1(yn5)* mutants were selected for further analysis. In a screen of 200 haploid genomes, we isolated one mutation, *yn39*, that enhanced and one mutation, *yn38*, that suppressed the lethality rate. The survival rate of those mutants was determined after several generations. For the enhancer strain, only 18% of its progeny survived at 27°, while the suppressor strain showed a 96% survival rate (Figure 5; Table 2). These modifying effects were not temperature dependent. At 20° *apl-1(yn5)* animals have a lethality rate of 14%, whereas *yn39*; *apl-1(yn5)* and *yn38*; *apl-1(yn5)* double mutants showed a lethality rate of 31 and 4%, respectively (Table 2). To determine whether the *yn39* enhancement of lethality is dependent on *apl-1(yn5)*, we outcrossed *yn39* from the *apl-1(yn5)* background, allowed F_2 animals to lay eggs, shifted F_3 eggs to 27°, and scored for survival after 44 hr. All eggs developed into L4 animals, suggesting that the *yn39* mutation by itself does not cause lethality but rather enhances the *apl-1(yn5)* lethality. As a control, from the same cross, 40 F_2 *apl-1(yn5)* heterozygous animals were also picked at 20°. Of the F_3 progeny, ~25% were homozygous for the *yn39* mutation (9/40 = 0–33% survival), while the rest of the animals showed a similar survival rate (40–60%) as *apl-1(yn5)* animals, except for one where 100% F_3 progeny survived, presumably due to recombination.

To determine whether the mutations suppressed or enhanced other *apl-1(yn5)* phenotypes, we examined L1 arrest. Both strains were outcrossed four times before phenotypic characterization and looked superficially wild type. The *yn38* mutation partially suppressed the L1 arrest, while the *yn39* enhanced the L1 arrest at 27°: *apl-1(yn5)* animals have an L1 arrest rate of 46%, whereas *yn39*; *apl-1(yn5)* and *yn38*; *apl-1(yn5)* double mutants showed L1 arrest rates of 69 and 23%, respectively (Figure S2; Table 2).

Both *yn38* and *yn39* are recessive alleles. *yn38* was mapped by conventional methods (Brenner 1974) to chromosome III and fine mapped using SNPs; *yn39* was mapped using SNPs to chromosome II. The DNA from both mutants was isolated and used for whole genome deep sequencing. Because both alleles were sequenced at the same time, we compared the DNA of each allele to wild type and to each other. For *yn38*, the deep sequencing revealed 41 variations on chromosome III compared to wild type. After subtracting those variations also found in the *yn39* sequence data, six candidate variations remained. One variant, R155.2, mapped to where fine SNP mapping predicted the mutation;

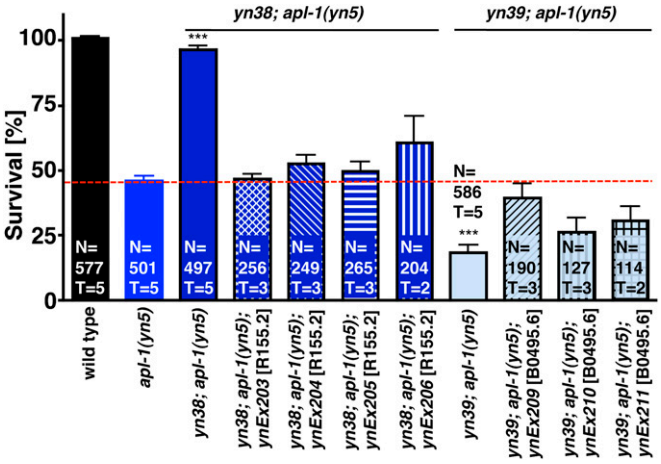

Figure 5 Suppressor and enhancer of the temperature-sensitive *apl-1 (yn5)* lethality. All wild-type eggs survived and developed into larval animals, whereas only 47% of *apl-1(yn5)* eggs survived and developed at 27°. From the mutagenesis screen, 96% of the *yn38*; *apl-1(yn5)* (dark blue bar) and 18% of the *yn39*; *apl-1(yn5)* (light blue bar) double mutant animals survived. The *yn38*; *apl-1(yn5)* and *yn39*; *apl-1(yn5)* survival rates were rescued to *apl-1(yn5)* rates in multiple independent transgenic lines carrying genomic fragments of MOA-1/R155.2 (dark blue hatched bars) and MOA-2/B0495.6 (light blue hatched bars), respectively. ***$P < 0.001$ to *apl-1(yn5)* determined with one-way ANOVA *post hoc* Tukey.

however, no RNAi clone was available in the Ahringer library for R155.2, which encodes a receptor protein tyrosine phosphatase (RPTP). RNAi knockdown of the remaining candidates revealed two candidates that phenocopied the increased survival of *yn38*; *apl-1(yn5)* animals (Figure S3). One candidate, *tag-235*, encodes a protein involved in endocytosis, and the second candidate, *dnj-24*, encodes a protein containing a DNA-J domain. To determine which candidate corresponds to *yn38*, wild-type DNA of these three candidates was microinjected into *yn38*; *apl-1(yn5)* mutants and tested for rescue by scoring the level of F_1 survival at 27°; only one candidate, R155.2 RPTP, showed rescue; we have named R155.2 *moa-1* (**mo**difier of ***a**pl-1*). All four independent transgenic lines of R155.2 reduced the 96% survival rates of *yn38*; *apl-1(yn5)* animals to an average of 52%, similar to the 47% survival rate of *apl-1(yn5)* mutants at 27° (Figure 5; Table S4). The missense mutation of *yn38* causes a threonine-to-isoleucine transition at amino acid 111 (T111I) in the extracellular domain of R155.2 RPTP, raising the possibility that the substitution disrupts ligand binding.

The deep sequencing of *yn39* revealed 42 variations on chromosome II compared to wild type. After subtracting those variations that overlapped with those of *yn38*, 15 candidate variations remained. RNAi knockdown of only 1 candidate, B0495.6, phenocopied the ~10% survival rate of *yn39*; *apl-1(yn5)* animals (Figure S3). Wild-type B0495.6 DNA was introduced into *yn39*; *apl-1(yn5)* and the three independent transgenic lines showed partial rescue by returning survival rates to an average of 32%, slightly lower than the 47% survival rate of *apl-1(yn5)* mutants (Figure 5;

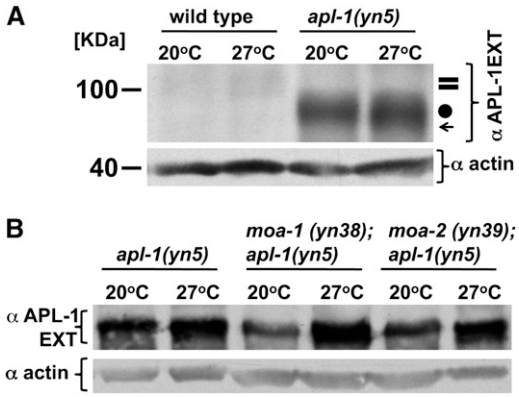

Figure 6 Protein levels of APL-1 are similar to *apl-1(yn5)* levels at 27°, but slightly decreased at 20° in the *moa-1*; *yn5* and *moa-2*; *yn5* mutants. (A and B) Western blots of extracts were probed with either an antiserum against the extracellular domain of APL-1 (αAPL-1EXT) or actin (α-actin). Animals were raised at the indicated temperature. (A) Double bar indicates the full-length glycosylated or unmodified APL-1, the circle indicates APL-1EXT, which corresponds to the entire extracellular domain of APL-1, and the arrow indicates sAPL-1, a cleavage product of APL-1 that is slightly smaller than APL-1EXT. (B) Relative intensities of APL-1 levels normalized to actin and levels in *apl-1(yn5)* extracts: *yn5* 20° 1; *yn5* 27° 0.88 ± 0.2; *moa-1(yn38)*; *apl-1(yn5)* 20° 0.49 ± 0.1; *moa-1(yn38)*; *apl-1(yn5)* 27° 0.96 ± 0.2; *moa-2(yn39)*; *apl-1(yn5)* 20° 0.69 ± 0.1; and *moa-2(yn39)*; *apl-1(yn5)* 27° 0.86 ± 0.2 (n = 2 trials; mean ± SEM are indicated). Molecular weight standards are indicated to the left.

Table S4). B0495.6, which we have named *moa-2*, encodes a protein of 87 amino acids; the *yn39* mutation is a deletion of 13 nucleotides, which leads to a frameshift after the 18th amino acid. B0495.6 has a splice factor 3B subunit domain (amino acids 6–26) and has been potentially implicated in receptor-mediated endocytosis (Balklava *et al.* 2007) and larval development (Kamath *et al.* 2003; Simmer *et al.* 2003; Sönnichsen *et al.* 2005).

To determine whether the *yn38* and *yn39* mutations affect the levels of APL-1EXT expression, we performed Western blots on extracts from *moa-1(yn38)*; *apl-1(yn5)* and *moa-2(yn39)*; *apl-1(yn5)* mutants raised at 20° and 27°. The levels of APL-1EXT increased slightly to *apl-1(yn5)* levels when the mutants were raised at 27° (Figure 6). Consequently, although the overall levels of APL-1EXT in *moa-1 (yn38)*; *apl-1(yn5)* and *moa-2(yn39)*; *apl-1(yn5)* mutants are less than that of *apl-1(yn5)* mutants at 20°, the APL-1EXT levels are similar at 27°, suggesting that suppression and enhancement of the *yn5* temperature-sensitive lethality by the *yn38* and *yn39* mutations, respectively, are not simply due to modulating the levels of APL-1EXT.

To analyze the genetic interaction between *moa-1* and *moa-2*, we used RNAi knockdown on *yn38* and *yn39* mutants. RNAi of either *dnj-24*, *tag-235*, or C08G5.1, which has off-target effects on R155.2, on *moa-2(yn39)*; *apl-1 (yn5)* animals did not alter the *yn39*; *apl-1(yn5)* lethality rate at 27° (Figure S3). Interestingly, feeding *yn38*; *apl-1 (yn5)* double mutants with *moa-2*/B0495.6 RNAi resulted in an F_2 synthetic lethality at 20° (three trials, number of F_1 animals >60), suggesting that *moa-1* and *moa-2* either function in the same pathway or in partially redundant pathways to affect development.

Discussion

Complete loss of *apl-1* causes a completely penetrant lethal molting defect during the first to second larval stage transition (Hornsten *et al.* 2007). We now show that *apl-1* knockdown by RNAi leads to a molting defect during all four larval stages (Wiese *et al.* 2010), indicating that *apl-1* is required for every larval molt. In addition, *apl-1(yn5)* mutants have a delayed development, suggesting that APL-1, and in particular sAPL-1, is involved in both developmental timing and the molting process, two processes that are intimately linked, but whose regulation can be genetically separated in *C. elegans* (Ruaud and Bessereau 2006; Monsalve *et al.* 2011), similar to the genetic separation of metamorphosis/molting and developmental timing in *Drosophila* (Thummel 2001). Interestingly, the metamorphosis/molting and developmental growth rate in *Drosophila* is regulated by the integrative action of insulin signaling via dFOXO and nuclear hormone receptor (ecdysone receptor) signaling (Colombani *et al.* 2005; Delanoue and Leopold 2010). In *C. elegans*, *daf-2* insulin/IGF-1 receptor and *daf-16* FOXO activity and TGFβ signaling pathway regulate expression of different collagen genes, which are necessary for stage-specific cuticles crucial during development (Yu and Larsen 2001; McElwee *et al.* 2004; Halaschek-Wiener *et al.* 2005; Ruzanov *et al.* 2007; Shaw *et al.* 2007;), but the pathways through which *daf-2*, *daf-16*, and *daf-12*, as well as *apl-1* act to affect the molting process is unclear. However, although the exact molecular pathway by which APL-1 activity affects DAF-2, DAF-16, and DAF-12 activity is unknown, our results demonstrate that *apl-1* activity requires the insulin, *daf-16* FOXO, and *daf-12* NHR pathways for multiple processes, including developmental progression, body length, and egg laying. We propose that after APL-1 cleavage, sAPL-1 signals to decrease insulin signaling to modulate DAF-16 function, thereby affecting developmental progression and metabolic functions regulating body length and reproduction. *daf-12* NHR integrates hormonal signaling with developmental timing by its position in the heterochronic feedback loop of *let-7* miRNA, which regulates late developmental progression from L4 to adults (Bethke *et al.* 2009; Hammell *et al.* 2009) and *apl-1* expression in seam cells (Niwa *et al.* 2008). RNAi knockdown of *daf-12* did not alter *apl-1* expression in seam cells during the late L4 stage (Hada *et al.* 2010) and possible miRNA binding sites in the 3′-UTR were deleted by the *apl-1(yn5)* mutation. Nevertheless, *daf-12* knockdown completely suppressed the developmental delay in *apl-1(yn5)* mutants. By contrast, the *daf-16 (mu86)* null mutation did not completely rescue the slowed development of *apl-1(yn5)* mutants, since a low percentage of *apl-1(yn5)*; *daf-16(mu86)* animals were still found in L1–L4 stages. Hence, *apl-1* activity may modulate the *daf-2* insulin/IGF-1 receptor pathway to affect or act in parallel with

the *daf-16* and *daf-12* pathways. Interestingly, this (these) signaling pathway(s) is (are) also observed to regulate different modalities, such as egg-laying behavior and body size. Similarly, transgenic *APP* mice show impairments in behavior, are lighter, and show reduced body weight gain compared to their wild-type littermates (Pugh *et al.* 2007; Codita *et al.* 2010). Weight loss is also associated with AD patients, despite the fact that AD patients consume more calories than age-matched non-AD controls (reviewed in Aziz *et al.* 2008), suggesting that AD patients may have altered metabolic rates (Wang *et al.* 2004). Our results suggest that metabolic rate changes could be mediated by secreted sAPP, which alters hormonal and insulin signaling pathways.

The temperature-sensitive lethality of *apl-1(yn5)* animals is not dependent on *daf-12* NHR or *daf-16* FOXO activity. We were somewhat surprised that screening such a small number of haploid genomes as well as RNAi clones identified during deep sequencing could identify modifiers of *apl-1* activity. These results suggest that APL-1 is involved in multiple pathways and/or that the *apl-1* pathway involves many genes. Our finding that decreased activity of MOA-1/R155.2 RPTP suppresses the *apl-1(yn5)* lethality suggests that either MOA-1/R155.2 RPTP is a receptor for sAPL-1 or that MOA-1/R155.2 RPTP is activated as a result of sAPL-1 signaling. *apl-1(yn5)* mutants contain high levels of APL-1EXT, which presumably increases downstream signaling through MOA-1/R155.2 RPTP. This downstream signaling could be further increased at 27°, leading to lethality; this situation may mimic overexpression of APL-1, which can also lead to lethality (Hornsten *et al.* 2007). The *yn38* mutation in *moa-1* could decrease the *apl-1(yn5)* lethality by decreasing receptor signaling. Many human RPTPs have similar tyrosine phosphatase domains as MOA-1/R155.2, but we found no similarities in the extracellular domain of MOA-1/R155.2 among human RPTPs with our BLAST searches. Alternatively, a second mechanism to decrease APL-1EXT signaling is to endocytose the bound or unbound receptor without affecting the levels of APL-1EXT; disruption of these endocytic pathways could either increase, such as with MOA-2/B0495.6, or decrease, such as *tag-235*, the *apl-1(yn5)* lethality, respectively. While the identification of *apl-1(yn5)* modifiers might correspond to a special situation with respect to the normal physiological function of APL-1, as the *apl-1(yn5)* mutants never express the cytoplasmic domain of APL-1, nevertheless, the extracellular domain of mammalian sAPPβ has previously been shown to act as a ligand for death receptor 6 (DR6) to initiate neurodegeneration (Nikolaev *et al.* 2009). Our results suggest that mammalian sAPP may also bind different receptors to differentially activate a cell death or neuronal survival pathway.

Acknowledgments

We thank Cathy Savage-Dunn's group for kindly providing their N2 strain; Alexander Boyanov together with Oliver Hobert's lab for whole genome sequencing of *yn38* and *yn39* mutants; Sarah Tichelli and Casey Brander for help with body length measurements; Mboutidem Etokakpan for help in the genetic screen; Piali Sengupta and Chip Ferguson for comments or helpful discussions on the manuscript; Li lab members for helpful discussions; and the *Caenorhabditis* Genetics Center, which is funded by the National Institutes of Health (NIH) National Center for Research Resources, for providing *daf-16*, DAF-16::GFP, and *daf-12* strains. This work was supported by grants from the Alzheimer's Association (IIRG-05-14190), NIH (R21AG033912 and R01AG032042), the National Science Foundation (IOS08207) (C.L.), and a NIH Research Centers in Minority Institutions grant (G12-RR03060) to the City College of New York.

Literature Cited

Abrahante, J. E., A. L. Daul, M. Li, M. L. Volk, J. M. Tennessen *et al.*, 2003 The *Caenorhabditis elegans* hunchback-like gene *lin-57/hbl-1* controls developmental time and is regulated by microRNAs. Dev. Cell 4: 625–637.

Ailion, M., and J. H. Thomas, 2000 Dauer formation induced by high temperatures in *Caenorhabditis elegans*. Genetics 156: 1047–1067.

Alzheimer's Association, 2010 2010 Alzheimer's disease facts and figures. Alzheimers Dement. 6: 158–194.

Antebi, A., W. H. Yeh, D. Tait, E. M. Hedgecock, and D. L. Riddle, 2000 *daf-12* encodes a nuclear receptor that regulates the dauer diapause and developmental age in *C. elegans*. Genes Dev. 14: 1512–1527.

Aziz, N. A., M. A. Van Der Marck, H. Pijl, M. G. Olde Rikkert, B. R. Bloem *et al.*, 2008 Weight loss in neurodegenerative disorders. J. Neurol. 255: 1872–1880.

Balklava, Z., S. Pant, H. Fares, and B. D. Grant, 2007 Genome-wide analysis identifies a general requirement for polarity proteins in endocytic traffic. Nat. Cell Biol. 9: 1066–1073.

Baugh, L. R., and P. W. Sternberg, 2006 DAF-16/FOXO regulates transcription of *cki-1*/Cip/Kip and repression of *lin-4* during *C. elegans* L1 arrest. Curr. Biol. 16: 780–785.

Bethke, A., N. Fielenbach, Z. Wang, D. J. Mangelsdorf, and A. Antebi, 2009 Nuclear hormone receptor regulation of microRNAs controls developmental progression. Science 324: 95–98.

Brenner, S., 1974 The Genetics of *Caenorhabditis elegans*. Genetics 77: 71–94.

Cabrejo, L., L. Guyant-Marechal, A. Laquerriere, M. Vercelletto, F. De La Fourniere *et al.*, 2006 Phenotype associated with *APP* duplication in five families. Brain 129: 2966–2976.

Caille, I., B. Allinquant, E. Dupont, C. Bouillot, A. Langer *et al.*, 2004 Soluble form of amyloid precursor protein regulates proliferation of progenitors in the adult subventricular zone. Development 131: 2173–2181.

Cassada, R. C., and R. L. Russell, 1975 The dauerlarva, a post-embryonic developmental variant of the nematode *Caenorhabditis elegans*. Dev. Biol. 46: 326–342.

Chartier-Harlin, M. C., F. Crawford, H. Houlden, A. Warren, D. Hughes *et al.*, 1991 Early-onset Alzheimer's disease caused by mutations at codon 717 of the beta-amyloid precursor protein gene. Nature 353: 844–846.

Church, D. L., K. L. Guan, and E. J. Lambie, 1995 Three genes of the MAP kinase cascade, *mek-2*, *mpk-1/sur-1* and *let-60 ras*, are required for meiotic cell cycle progression in *Caenorhabditis elegans*. Development 121: 2525–2535.

Codita, A., A. Gumucio, L. Lannfelt, P. Gellerfors, B. Winblad *et al.*, 2010 Impaired behavior of female tg-ArcSwe APP mice in the IntelliCage: A longitudinal study. Behav. Brain Res. 215: 83–94.

Colombani, J., L. Bianchini, S. Layalle, E. Pondeville, C. Dauphin-Villemant *et al.*, 2005 Antagonistic actions of ecdysone and insulins determine final size in *Drosophila*. Science 310: 667–670.

Curran, S. P., and G. Ruvkun, 2007 Lifespan regulation by evolutionarily conserved genes essential for viability. PLoS Genet. 3: e56.

Daigle, I., and C. Li, 1993 *apl-1*, a *Caenorhabditis elegans* gene encoding a protein related to the human beta-amyloid protein precursor. Proc. Natl. Acad. Sci. USA 90: 12045–12049.

Davis, M. W., M. Hammarlund, T. Harrach, P. Hullett, S. Olsen *et al.*, 2005 Rapid single nucleotide polymorphism mapping in *C. elegans*. BMC Genomics 6: 118.

Delanoue, R., and P. Leopold, 2010 Developmental biology: a DOR connecting growth and clocks. Curr. Biol. 20: R884–R886.

Fielenbach, N., and A. Antebi, 2008 *C. elegans* dauer formation and the molecular basis of plasticity. Genes Dev. 22: 2149–2165.

Gems, D., A. J. Sutton, M. L. Sundermeyer, P. S. Albert, K. V. King *et al.*, 1998 Two pleiotropic classes of *daf-2* mutation affect larval arrest, adult behavior, reproduction and longevity in *Caenorhabditis elegans*. Genetics 150: 129–155.

Goate, A., M. C. Chartier-Harlin, M. Mullan, J. Brown, F. Crawford *et al.*, 1991 Segregation of a missense mutation in the amyloid precursor protein gene with familial Alzheimer's disease. Nature 349: 704–706.

Gralle, M., and S. T. Ferreira, 2007 Structure and functions of the human amyloid precursor protein: the whole is more than the sum of its parts. Prog. Neurobiol. 82: 11–32.

Grosshans, H., T. Johnson, K. L. Reinert, M. Gerstein, and F. J. Slack, 2005 The temporal patterning microRNA *let-7* regulates several transcription factors at the larval to adult transition in *C. elegans*. Dev. Cell 8: 321–330.

Hada, K., M. Asahina, H. Hasegawa, Y. Kanaho, F. J. Slack *et al.*, 2010 The nuclear receptor gene *nhr-25* plays multiple roles in the *Caenorhabditis elegans* heterochronic gene network to control the larva-to-adult transition. Dev. Biol. 344: 1100–1109.

Halaschek-Wiener, J., J. S. Khattra, S. Mckay, A. Pouzyrev, J. M. Stott *et al.*, 2005 Analysis of long-lived *C. elegans daf-2* mutants using serial analysis of gene expression. Genome Res. 15: 603–615.

Hammell, C. M., X. Karp, and V. Ambros, 2009 A feedback circuit involving *let-7*-family miRNAs and DAF-12 integrates environmental signals and developmental timing in *Caenorhabditis elegans*. Proc. Natl. Acad. Sci. USA 106: 18668–18673.

Heber, S., J. Herms, V. Gajic, J. Hainfellner, A. Aguzzi *et al.*, 2000 Mice with combined gene knock-outs reveal essential and partially redundant functions of amyloid precursor protein family members. J. Neurosci. 20: 7951–7963.

Henderson, S. T., and T. E. Johnson, 2001 *daf-16* integrates developmental and environmental inputs to mediate aging in the nematode *Caenorhabditis elegans*. Curr. Biol. 11: 1975–1980.

Herms, J., B. Anliker, S. Heber, S. Ring, M. Fuhrmann *et al.*, 2004 Cortical dysplasia resembling human type 2 lissencephaly in mice lacking all three APP family members. EMBO J. 23: 4106–4115.

Hoopes, J. T., X. Liu, X. Xu, B. Demeler, E. Folta-Stogniew *et al.*, 2010 Structural characterization of the E2 domain of APL-1, a *Caenorhabditis elegans* homolog of human amyloid precursor protein, and its heparin binding site. J. Biol. Chem. 285: 2165–2173.

Hornsten, A., J. Lieberthal, S. Fadia, R. Malins, L. Ha *et al.*, 2007 APL-1, a *Caenorhabditis elegans* protein related to the human beta-amyloid precursor protein, is essential for viability. Proc. Natl. Acad. Sci. USA 104: 1971–1976.

Jeong, M. H., I. Kawasaki, and Y. H. Shim, 2010 A circulatory transcriptional regulation among *daf-9*, *daf-12*, and *daf-16* mediates larval development upon cholesterol starvation in *Caenorhabditis elegans*. Dev. Dyn. 239: 1931–1940.

Kamath, R. S., M. Martinez-Campos, P. Zipperlen, A. G. Fraser, and J. Ahringer, 2001 Effectiveness of specific RNA-mediated interference through ingested double-stranded RNA in *Caenorhabditis elegans*. Genome Biol. 2: RESEARCH0002.

Kamath, R. S., A. G. Fraser, Y. Dong, G. Poulin, R. Durbin *et al.*, 2003 Systematic functional analysis of the *Caenorhabditis elegans* genome using RNAi. Nature 421: 231–237.

Kang, J., H. G. Lemaire, A. Unterbeck, J. M. Salbaum, C. L. Masters *et al.*, 1987 The precursor of Alzheimer's disease amyloid A4 protein resembles a cell-surface receptor. Nature 325: 733–736.

Kidd, M., 1964 Alzheimer's Disease: an electron microscopical study. Brain 87: 307–320.

Kimura, K. D., H. A. Tissenbaum, Y. Liu, and G. Ruvkun, 1997 *daf-2*, an insulin receptor-like gene that regulates longevity and diapause in *Caenorhabditis elegans*. Science 277: 942–946.

Klass, M., and D. Hirsh, 1976 Non-ageing developmental variant of *Caenorhabditis elegans*. Nature 260: 523–525.

Krigman, M. R., R. G. Feldman, and K. Bensch, 1965 Alzheimer's presenile dementia. A histochemical and electron microscopic study. Lab. Invest. 14: 381–396.

Kuester, M., S. Kemmerzehl, S. O. Dahms, D. Roeser, and M. E. Than, 2011 The crystal structure of death receptor 6 (DR6): a potential receptor of the amyloid precursor protein (APP). J. Mol. Biol. 409: 189–201.

Larsen, P. L., 1993 Aging and resistance to oxidative damage in *Caenorhabditis elegans*. Proc. Natl. Acad. Sci. USA 90: 8905–8909.

Larsen, P. L., P. S. Albert, and D. L. Riddle, 1995 Genes that regulate both development and longevity in *Caenorhabditis elegans*. Genetics 139: 1567–1583.

Lee, R. Y., J. Hench, and G. Ruvkun, 2001 Regulation of *C. elegans* DAF-16 and its human ortholog FKHRL1 by the *daf-2* insulin-like signaling pathway. Curr. Biol. 11: 1950–1957.

Lin, K., J. B. Dorman, A. Rodan, and C. Kenyon, 1997 *daf-16*: an HNF-3/forkhead family member that can function to double the life-span of *Caenorhabditis elegans*. Science 278: 1319–1322.

Lin, K., H. Hsin, N. Libina, and C. Kenyon, 2001 Regulation of the *Caenorhabditis elegans* longevity protein DAF-16 by insulin/IGF-1 and germline signaling. Nat. Genet. 28: 139–145.

Lithgow, G. J., T. M. White, S. Melov, and T. E. Johnson, 1995 Thermotolerance and extended life-span conferred by single-gene mutations and induced by thermal stress. Proc. Natl. Acad. Sci. USA 92: 7540–7544.

Luse, S. A., and K. R. Smith Jr., 1964 The ultrastructure of senile plaques. Am. J. Pathol. 44: 553–563.

Mattson, M. P., 1997 Cellular actions of beta-amyloid precursor protein and its soluble and fibrillogenic derivatives. Physiol. Rev. 77: 1081–1132.

McElwee, J. J., E. Schuster, E. Blanc, J. H. Thomas, and D. Gems, 2004 Shared transcriptional signature in *Caenorhabditis elegans* Dauer larvae and long-lived *daf-2* mutants implicates detoxification system in longevity assurance. J. Biol. Chem. 279: 44533–44543.

Monsalve, G. C., C. Van Buskirk, and A. R. Frand, 2011 LIN-42/PERIOD controls cyclical and developmental progression of *C. elegans* molts. Curr. Biol. 21: 2033–2045.

Murrell, J., M. Farlow, B. Ghetti, and M. D. Benson, 1991 A mutation in the amyloid precursor protein associated with hereditary Alzheimer's disease. Science 254: 97–99.

Narasimhan, S. D., K. Yen, A. Bansal, E. S. Kwon, S. Padmanabhan *et al.*, 2011 PDP-1 links the TGF-beta and IIS pathways to regulate longevity, development, and metabolism. PLoS Genet. 7: e1001377.

Nikolaev, A., T. Mclaughlin, D. D. O'leary, and M. Tessier-Lavigne, 2009 APP binds DR6 to trigger axon pruning and neuron death via distinct caspases. Nature 457: 981–989.

Niwa, R., F. Zhou, C. Li, and F. J. Slack, 2008 The expression of the Alzheimer's amyloid precursor protein-like gene is regulated by developmental timing microRNAs and their targets in *Caenorhabditis elegans*. Dev. Biol. 315: 418–425.

Ogg, S., S. Paradis, S. Gottlieb, G. I. Patterson, L. Lee *et al.*, 1997 The Fork head transcription factor DAF-16 transduces insulin-like metabolic and longevity signals in *C. elegans*. Nature 389: 994–999.

Pugh, P. L., J. C. Richardson, S. T. Bate, N. Upton, and D. Sunter, 2007 Non-cognitive behaviours in an APP/PS1 transgenic model of Alzheimer's disease. Behav. Brain Res. 178: 18–28.

Resnick, T. D., K. A. Mcculloch, and A. E. Rougvie, 2010 miRNAs give worms the time of their lives: small RNAs and temporal control in *Caenorhabditis elegans*. Dev. Dyn. 239: 1477–1489.

Riddle, D. L., M. M. Swanson, and P. S. Albert, 1981 Interacting genes in nematode dauer larva formation. Nature 290: 668–671.

Rossjohn, J., R. Cappai, S. C. Feil, A. Henry, W. J. Mckinstry *et al.*, 1999 Crystal structure of the N-terminal, growth factor-like domain of Alzheimer amyloid precursor protein. Nat. Struct. Biol. 6: 327–331.

Roush, S. F., and F. J. Slack, 2009 Transcription of the *C. elegans let-7* microRNA is temporally regulated by one of its targets, *hbl-1*. Dev. Biol. 334: 523–534.

Rovelet-Lecrux, A., D. Hannequin, G. Raux, N. Le Meur, A. Laquerriere *et al.*, 2006 *APP* locus duplication causes autosomal dominant early-onset Alzheimer disease with cerebral amyloid angiopathy. Nat. Genet. 38: 24–26.

Ruaud, A. F., and J. L. Bessereau, 2006 Activation of nicotinic receptors uncouples a developmental timer from the molting timer in *C. elegans*. Development 133: 2211–2222.

Ruzanov, P., D. L. Riddle, M. A. Marra, S. J. Mckay, and S. M. Jones, 2007 Genes that may modulate longevity in *C. elegans* in both dauer larvae and long-lived *daf-2* adults. Exp. Gerontol. 42: 825–839.

Sarin, S., V. Bertrand, H. Bigelow, A. Boyanov, M. Doitsidou *et al.*, 2010 Analysis of multiple ethyl methanesulfonate-mutagenized *Caenorhabditis elegans* strains by whole-genome sequencing. Genetics 185: 417–430.

Savage-Dunn, C., L. L. Maduzia, C. M. Zimmerman, A. F. Roberts, S. Cohen *et al.*, 2003 Genetic screen for small body size mutants in *C. elegans* reveals many TGFbeta pathway components. Genesis 35: 239–247.

Schmitz, A., R. Tikkanen, G. Kirfel, and V. Herzog, 2002 The biological role of the Alzheimer amyloid precursor protein in epithelial cells. Histochem. Cell Biol. 117: 171–180.

Shaw, W. M., S. Luo, J. Landis, J. Ashraf, and C. T. Murphy, 2007 The *C. elegans* TGF-beta Dauer pathway regulates longevity via insulin signaling. Curr. Biol. 17: 1635–1645.

Simmer, F., C. Moorman, A. Van Der Linden, E. Kuijk, P. V. Van Den Berghe *et al.*, 2003 Genome-wide RNAi of *C. elegans* using the hypersensitive *rrf-3* strain reveals novel gene functions. PLoS Biol. 1: E12.

Slack, F. J., M. Basson, Z. Liu, V. Ambros, H. R. Horvitz *et al.*, 2000 The *lin-41* RBCC gene acts in the *C. elegans* heterochronic pathway between the *let-7* regulatory RNA and the LIN-29 transcription factor. Mol. Cell 5: 659–669.

Sleegers, K., N. Brouwers, I. Gijselinck, J. Theuns, D. Goossens *et al.*, 2006 *APP* duplication is sufficient to cause early onset Alzheimer's dementia with cerebral amyloid angiopathy. Brain 129: 2977–2983.

So, S., K. Miyahara, and Y. Ohshima, 2011 Control of body size in *C. elegans* dependent on food and insulin/IGF-1 signal. Genes Cells 16: 639–651.

Sönnichsen, B., L. B. Koski, A. Walsh, P. Marschall, B. Neumann *et al.*, 2005 Full-genome RNAi profiling of early embryogenesis in *Caenorhabditis elegans*. Nature 434: 462–469.

Sulston, J. E., and H. R. Horvitz, 1977 Post-embryonic cell lineages of the nematode, *Caenorhabditis elegans*. Dev. Biol. 56: 110–156.

Sulston, J. E., E. Schierenberg, J. G. White, and J. N. Thomson, 1983 The embryonic cell lineage of the nematode *Caenorhabditis elegans*. Dev. Biol. 100: 64–119.

Tennessen, J. M., K. J. Opperman, and A. E. Rougvie, 2010 The *C. elegans* developmental timing protein LIN-42 regulates diapause in response to environmental cues. Development 137: 3501–3511.

Terry, R. D., N. K. Gonatas, and M. Weiss, 1964 Ultrastructural studies in Alzheimer's presenile dementia. Am. J. Pathol. 44: 269–297.

Thummel, C. S., 2001 Molecular mechanisms of developmental timing in *C. elegans* and *Drosophila*. Dev. Cell 1: 453–465.

Vowels, J. J., and J. H. Thomas, 1992 Genetic analysis of chemosensory control of dauer formation in *Caenorhabditis elegans*. Genetics 130: 105–123.

Wang, P. N., C. L. Yang, K. N. Lin, W. T. Chen, L. C. Chwang *et al.*, 2004 Weight loss, nutritional status and physical activity in patients with Alzheimer's disease. A controlled study. J. Neurol. 251: 314–320.

Wiese, M., A. Antebi, and H. Zheng, 2010 Intracellular trafficking and synaptic function of APL-1 in *Caenorhabditis elegans*. PLoS ONE 5**:** e12790.

Yu, H., and P. L. Larsen, 2001 DAF-16-dependent and independent expression targets of DAF-2 insulin receptor-like pathway in *Caenorhabditis elegans* include FKBPs. J. Mol. Biol. 314: 1017–1028.

Zambrano, N., M. Bimonte, S. Arbucci, D. Gianni, T. Russo *et al.*, 2002 *feh-1* and *apl-1*, the *Caenorhabditis elegans* orthologues of mammalian Fe65 and beta-amyloid precursor protein genes, are involved in the same pathway that controls nematode pharyngeal pumping. J. Cell Sci. 115: 1411–1422.

Zheng, H., M. Jiang, M. E. Trumbauer, D. J. Sirinathsinghji, R. Hopkins *et al.*, 1995 beta-Amyloid precursor protein-deficient mice show reactive gliosis and decreased locomotor activity. Cell 81: 525–531.

Communicating editor: K. Kemphues

GENETICS

Supporting Information
http://www.genetics.org/content/suppl/2012/03/30/genetics.112.138768.DC1

APL-1, the Alzheimer's Amyloid Precursor Protein in *Caenorhabditis elegans*, Modulates Multiple Metabolic Pathways Throughout Development

Collin Y. Ewald, Daniel A. Raps, and Chris Li

DOI: 10.1534/genetics.112.138768

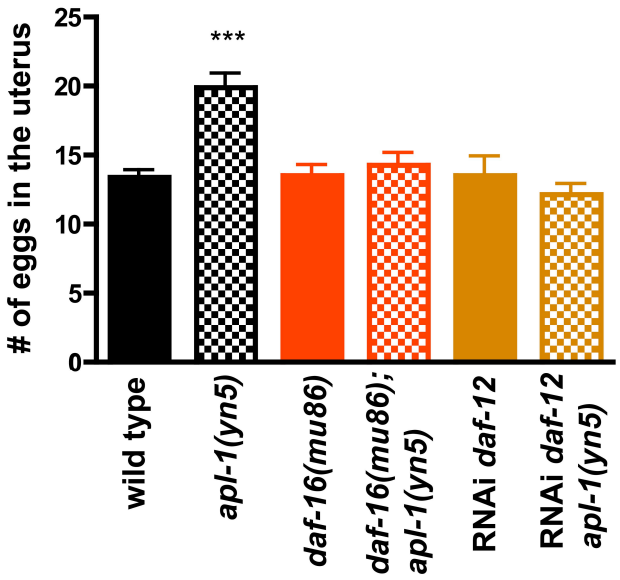

Figure S1 *apl-1(yn5)* mutants retain eggs in the uterus, but this phenotype can be suppressed by loss of *daf-16* FOXO and *daf-12* activity. The number of eggs retained in the uterus of two-day-old adult *C. elegans* hermaphrodites was scored. *apl-1(yn5)* mutants retain more eggs compared to wild-type animals. *daf-16(mu86)*; *apl-1(yn5)* double mutants have similar numbers of eggs in their uterus as *daf-16(mu86)* null mutants or wild-type animals. Three trials, N>30, except for strains in which *daf-12* was inactivated by RNAi (one trial, N=12). ***=P<0.001 determined by one-way ANOVA with Tukey post-test.

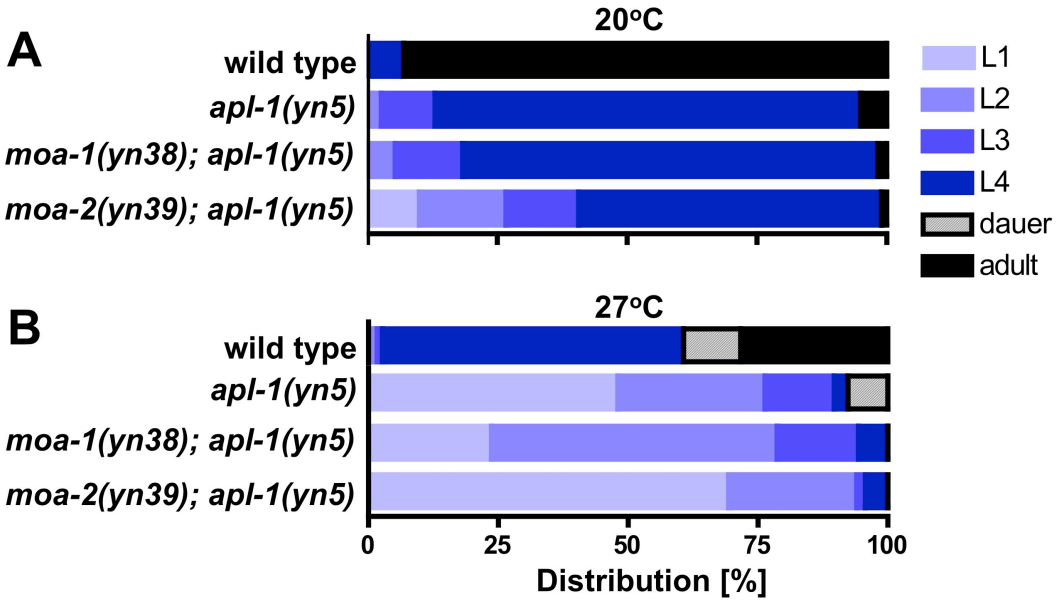

Figure S2 APL-1 overexpression animals arrest as first larval stage animals at higher temperatures. **A.** At 20°C, most wild-type eggs developed into adults after 72 hours. By contrast, *apl-1(yn5)* mutants are found at earlier larval stages. **B.** At 27°C, most wild-type eggs developed into L4 or adults and about 10% went into diapause after 44 hours. By contrast, 50% of the surviving *apl-1(yn5)* mutant arrested in the L1 stage, 40% progressed to L2-L4, and 10% became dauer animals. Strikingly, about 90% of animals with pan-neuronal APL-1 overexpression were found in the L1 stage. For N values see Table 2; *Is,* [] indicates integrated transgene.

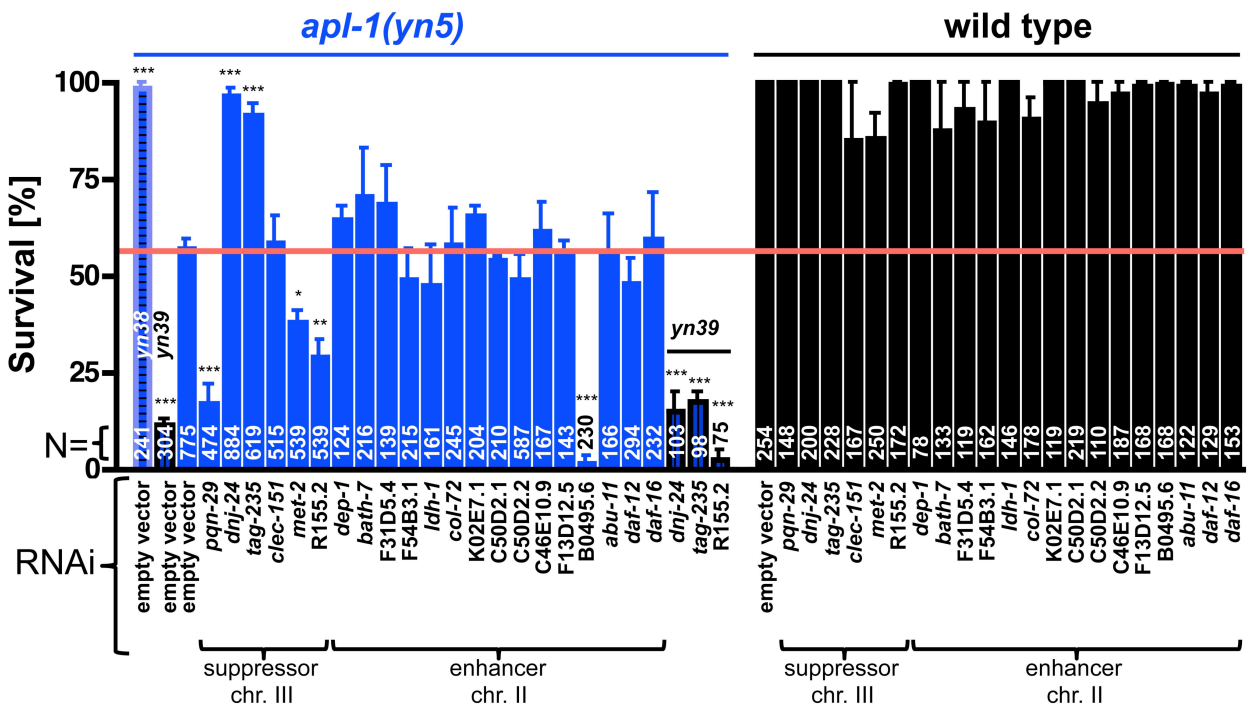

Figure S3 RNAi knockdown of *dnj-24*, *tag-235*, and *moa-2*/B0495.6 modified the survival rate of *apl-1(yn5)* mutants at 27°C. Wild-type animals (in black) or *apl-1(yn5)* mutants (in blue) were grown on RNAi plates for two generations. F2 adults were allowed to lay eggs at 20°C, the F3 eggs were shifted to 27°C, and then scored for survival at 27°C after 72 hours. Knockdown of two candidate suppressor genes (*dnj-24* and *tag-235*) phenocopied the survival rates of *yn38; apl-1(yn5)* double mutants. The RNAi clone II-IM10 targets C08G5.1, a predicted peptidase, and has off-target effects on MOA-1/ R155.2; knockdown with II-IM10 failed to phenocopy the survival of *yn38; apl-1(yn5)* double mutants. Knockdown of only one candidate enhancer gene (B0495.6) on *apl-1(yn5)* mutants phenocopied the survival of *yn39; apl-1(yn5)* double mutants. RNAi of *daf-12*, *daf-16* or *abu-11* (Activated in Blocked Unfolded protein response) did not affect the survival of *apl-1(yn5)* mutants. RNAi of suppressor candidates (*dnj-24, tag-235*, R155.2 on *yn39; apl-1(yn5)* double mutants did not alter *yn39; apl-1(yn5)* survival rate at 27°C. All RNAi knockdowns on wild type did not affect their survival rate at 27°C. Trials >3. Chr., chromosome. *=P<0.05, **=P<0.01,***=P<0.001 determined by one-way ANOVA with Tukey post-test.

LITERATURE CITED IN SUPPORTING INFORMATION

CURRAN, S. P., and G. RUVKUN, 2007 Lifespan regulation by evolutionarily conserved genes essential for viability. PLoS Genet **3:** e56.

Table S1 DAF-16::GFP nuclear translocation upon 35°C heat stress is delayed by *apl-1(yn5)* activity

Strains	Cumulative distribution [%] in categories				N (T)
	0	**1**	**2**	**3**	
0 minutes at 35°C					
zIs356 [DAF-16::GFP]	100	0	0	0	176 (7)
zIs356; apl-1(yn5)	100	0	0	0	107 (1)
zIs356; *ynIs106* [APL-1EXT*(yn32)*]	100	0	0	0	32 (1)
zIs356 flp-1(ok2781)	100	0	0	0	27 (1)
30 minutes at 35°C					
zIs356 [DAF-16::GFP]	93	7	0	0	329 (12)
zIs356; apl-1(yn5)	100	0	0	0	127 (4)
zIs356; *ynIs106* [APL-1EXT*(yn32)*]	97.5	2.5	0	0	61 (1)
zIs356 flp-1(ok2781)	97	3	0	0	33 (1)
60 minutes at 35°C					
zIs356 [DAF-16::GFP]	0	100	0	0	245 (10)
zIs356; apl-1(yn5)	11	89	0	0	141 (4)
zIs356; *ynIs106* [APL-1EXT*(yn32)*]	0	100	0	0	33 (1)
zIs356 flp-1(ok2781)	0	100	0	0	63 (1)
90 minutes at 35°C					
zIs356 [DAF-16::GFP]	0	7	91	2	255 (9)
zIs356; apl-1(yn5)	0	93	7	0	150 (4) #
zIs356; *ynIs106* [APL-1EXT*(yn32)*]	0	0	100	0	53 (1)
zIs356 flp-1(ok2781)	0	0	100	0	30 (1)
120 minutes at 35°C					
zIs356 [DAF-16::GFP]	0	0	84	16	445 (8)
zIs356; apl-1(yn5)	0	84	16	0	141 (3) #
zIs356; *ynIs106* [APL-1EXT*(yn32)*]	0	0	7	93	40 (1)
zIs356; *flp-1(ok2781)*	0	0	39	61	41 (1)
150 minutes at 35°C					
zIs356 [DAF-16::GFP]	0	0	13	87	518 (9)
zIs356; apl-1(yn5)	0	0	97	3	156 (3) #
zIs356; *ynIs106* [APL-1EXT*(yn32)*]	0	0	3	97	38 (1)
zIs356 flp-1(ok2781)	0	0	9	91	12 (1)

DAF-16::GFP localization was scored on synchronized 1 day old adults. N corresponds to number of worms observed. T corresponds to number of independent trials. The rate of DAF-16::GFP nuclear translocation was scored as described (CURRAN and RUVKUN 2007): category 0: all DAF-16::GFP showing diffuse localization in the cytoplasm; category 1: more DAF-16::GFP localized in cytoplasm than in nucleus; category 2: more DAF-16::GFP localized in nucleus than in cytoplasm; category 3: almost all DAF-16::GFP localized in nucleus. *Is*, [] integrated transgene; transgenes were driven by the *apl-1* promoter unless otherwise noted; the encoded protein is indicated; DAF-16::GFP is driven by the *daf-16* promoter. *apl-1(yn32)* is a missense mutation that corresponds to a null allele. *flp-1(ok2781)* was used as another control. For statistical analysis: P-values were determined by χ^2 (3 degrees of freedom) and are only indicated by (#) when P<0.001 against *zIs356* [DAF-16::GFP].

Table S2 *apl-1(yn5)* mutants have a small body size that requires *daf-16* and *daf-12* activity

Strain (Genotype)	Length ± S.E.M. [μm]	N	% N2	P-Value against N2	P-Value against control ($^{◊,^,\#,@}$)
wild type (N2)	1225 ± 6.6	172			>0.05$^{◊}$
ynIs100 [APL-1*(yn32)*::GFP]	1200 ± 21.3	20	-2%	>0.05	>0.05$^{◊}$
ynIs86 [APL-1]	1074 ± 11.9	59	-12%	<0.001	<0.001$^{◊}$
ynIs79 [APL-1::GFP]	986 ± 9.6	89	-20%	<0.001	<0.001$^{◊}$
apl-1(yn10) {APL-1}	1016 ± 19.3	46	-17%	<0.001	<0.001$^{◊}$
apl-1(yn5)	1047 ± 11.6	63	-15%	<0.001	<0.001$^{◊}$
ynIs71 [APL-1EXT]	894 ± 28.2	33	-27%	<0.001	<0.001$^{◊}$
daf-16(mu86)	1263 ± 15.8	45	+3%	>0.05	
daf-16(mu86); ynIs79 [APL-1::GFP]	1247 ± 10.2	34	+2%	>0.05	>0.05$^{◊}$
daf-16(mu86); apl-1(yn5)	1243 ± 9.0	99	+1%	>0.05	>0.05$^{◊}$
daf-2(e1370)	1131 ± 9.4	44	-8%	<0.001	<0.001$^{◊}$
daf-2(e1370); apl-1(yn5)	991 ± 15.2	30	-19%	<0.001	<0.01^
daf-2(e1370); ynIs79 [APL-1::GFP]	1037 ± 12.0	51	-15%	<0.001	<0.01^
daf-2(e1370); apl-1(yn10) {APL-1}	1228 ± 15.8	17	0%	>0.05	>0.05^
daf-2(e1370); daf-16(mu86)	1250 ± 9.9	31	+2%	>0.05	>0.05$^{◊}$
daf-2(e1370); daf-16(mu86); apl-1(yn5)	1249 ± 12.3	33	+2%	>0.05	>0.05$^{◊}$
zIs356 [DAF-16::GFP]*	1124 ± 20.8	15	-8%	>0.05	<0.01$^{◊}$
zIs356; *ynIs79* [APL-1::GFP]*	1034 ± 12.2	29	-16%	<0.001	>0.05$^{\#}$
daf-12(m20)	1173 ± 11.8	45	-4%	>0.05	<0.05$^{◊}$
daf-12(m20); ynIs71 [APL-1EXT]	1196 ± 16.8	64	-2%	>0.05	>0.05$^{@}$
N2 grown on L4440 RNAi	1345 ± 15.2	51			
N2 grown on *daf-12* RNAi	1337 ± 14.6	28	-1%$^{∞}$	>0.05$^{∞}$	<0.05$^{»}$
apl-1(yn5) grown on L4440 RNAi	1254 ± 18.3	35	-7%$^{∞}$	<0.01$^{∞}$	
apl-1(yn5) grown on *daf-12* RNAi	1476 ± 20.9	36	+10%$^{∞}$	<0.001$^{∞}$	<0.001$^{»}$

Three day old adults were scored. SUR-5::GFP was used as a co-injection marker for *ynIs71* and *ynIs86* and *rol-6(su1006* for *ynIs79* and *ynIs100. Is*, [] integrated transgene. *Ex*, {} non-integrated transgene. Transgenes were driven by the *apl-1* promoter unless otherwise noted; the encoded protein is indicated; DAF-16::GFP is driven by the *daf-16* promoter. (N) corresponds to the number of animals observed. L4440 RNAi = empty vector control. P-values were determined by one-way ANOVAs with Tukey post-test (95% confidence intervals). P values against controls: **◊** = *daf-16(mu86)*, **^** = *daf-2(e1370)*, **#** = *zIs356* [DAF-16::GFP], *@* = *daf-12(m20)*, ∞ = N2 grown on L4440 RNAi, » = *apl-1(yn5)* grown on L4440 RNAi. Because data from the N2 strains from our lab and those from the lab of Cathy Savage-Dunn showed no statistical difference, the N2 body size statistics were combined.

Table S3 ***apl-1(yn5)*** **mutants have a decreased egg-laying-rate that is dependent on** ***daf-16*** **activity**

Strain (Genotype)	N_{Po}	T	N_{eggs}	Average Egg/1h/1Po ± S.E.M.	% N2	P-value against N2	P-value against control ($^{\lozenge,\wedge,\#,@}$)
wild type (N2)	988	38	10156	7.3 ± 0.3			>0.05$^{\lozenge}$
lon-2(e678) apl-1(yn10)/dpy-8(e130)	52	4	113	3.4 ± 1.3	-53%	>0.05	0.0084
ynIs100 [APL-1(*yn32*)::GFP]	83	3	575	5.4 ± 0.9	-26%	>0.05	0.0188
ynIs107 [APL-1(*yn32*)D342C/S362C::GFP]	118	6	994	7.9 ± 1.0	+8%	>0.05	0.5892
ynIs86 [APL-1]	173	5	1718	4.7 ± 0..6	-36%	<0.05	0.0017
ynIs79 [APL-1::GFP]	609	16	4214	4.5 ± 0.3	-38%	<0.001	<0.0001
apl-1(yn5)	1055	34	7118	4.3 ± 0.2	-41%	<0.001	<0.0001
ynIs71 [APL-1EXT]	291	6	2693	4.7 ± 0.5	-36%	<0.05	0.0008
daf-16(mu86)	136	10	1631	8.5 ± 0.6	+16%	>0.05	
daf-16(mu86); ynIs86	78	4	557	8.6 ± 0.8	+18%	>0.05	>0.05$^{\lozenge}$
daf-16(mu86); ynIs79	92	4	1274	9.1 ± 0.7	+25%	<0.05	>0.05$^{\lozenge}$
daf-16(mu86); apl-1(yn5)	199	4	1272	8.5 ± 0.9	+16%	>0.05	>0.05$^{\lozenge}$
zIs356 [DAF-16::GFP]	276	9	2092	1.4 ± 0.1	-81%	<0.001	<0.001$^{\lozenge}$
zIs356; *ynIs79*	295	7	2633	1.5 ± 0.1	-79%	<0.001	>0.05$^{\#}$
zIs356; *apl-1(yn5)*	121	3	1165	2.9 ± 0.3	-60%	<0.001	>0.05$^{\#}$
daf-12(m20)	86	7	936	7.1 ± 0.5	-3%	>0.05	>0.05$^{\lozenge}$
daf-12(m20); ynIs71	53	5	724	7.2 ± 0.2	-1%	>0.05	>0.05$^{@}$

Two day old adults were scored at room temperature (22-24^{o}C). All developmental distributions are shown in cumulative form. SUR-5::GFP was used as a co-injection marker for *ynIs71* and *ynIs86* and *rol-6(su1006)* for *ynIs79* and *ynIs100*. *Is*, [] integrated transgene, *Ex*, {} non-integrated transgene. Transgenes were driven by the *apl-1* promoter unless otherwise noted; the encoded protein is indicated; DAF-16::GFP is driven by the *daf-16* promoter. (N) corresponds to the number of animals observed. (T) corresponds to the number of independent times experiment was performed. P-values were determined by one-way ANOVAs with Tukey post-test (95% confidence intervals). P values against controls: **◊** = *daf-16(mu86)*, **#** = *zIs356* [DAF-16::GFP], @ = *daf-12(m20)*. Because data from the N2 strains from our lab and those from the lab of Cathy Savage-Dunn showed no statistical difference, the N2 egg-laying rate statistics were combined.

Table S4 Rescue of *yn38* and *yn39* mutations to *apl-1(yn5)* survival rates at 27°C

Strain (Genotype	N_{eggs}	GFP transmission at 20°C	GFP transmission at 27°C	Observed survival	Expected survival
Trial 1					
wild type (N2)	195	-	-	100	100
apl-1(yn5)	54	-	-	39	40-50
yn38; apl-1(yn5)	114	-	-	98	90-100
yn38; apl-1(yn5); ynEx201 [TAG-235]	80	44	59	95	72
yn38; apl-1(yn5); ynEx202 [TAG-235]	46	59	67	92	63
yn38; apl-1(yn5); ynEx207 [DNJ-24]	105	44	66	87	71
yn38; apl-1(yn5); ynEx208 [DNJ-24]	54	58	60	93	63
yn38; apl-1(yn5); ynEx203 [R155.2]	27	75	16	44	52
yn38; apl-1(yn5); ynEx204 [R155.2]	134	74	19	49	54
yn38; apl-1(yn5); ynEx205 [R155.2]	39	78	12	44	51
yn38; apl-1(yn5); ynEx206 [R155.2]	106	70	7	50	56
yn39; apl-1(yn5)	40	-	-	15	10-20
yn39; apl-1(yn5); ynEx209 [B0495.6]	98	50	72	35	27
yn39; apl-1(yn5); ynEx210 [B0495.6]	69	77	62	25	33
yn39; apl-1(yn5); ynEx211 [B0495.6]	53	67	66	36	31
Trial 2					
wild type (N2)	159	-	-	98	100
apl-1(yn5)	111	-	-	36	40-50
yn38; apl-1(yn5)	85	-	-	100	90-100
yn38; apl-1(yn5); ynEx201 [TAG-235]	44	73	46	100	53
yn38; apl-1(yn5); ynEx202 [TAG-235]	24	74	30	96	53
yn38; apl-1(yn5); ynEx207 [DNJ-24]	27	61	74	85	61
yn38; apl-1(yn5); ynEx208 [DNJ-24]	42	71	62	69	55
yn38; apl-1(yn5); ynEx203 [R155.2]	105	76	13	50	51
yn38; apl-1(yn5); ynEx204 [R155.2]	41	73	0	59	53
yn38; apl-1(yn5); ynEx205 [R155.2]	69	68	20	56	57
yn39; apl-1(yn5)	125	-	-	10	10-20
yn39; apl-1(yn5); ynEx209 [B0495.6]	14	68	71	50	28
yn39; apl-1(yn5); ynEx210 [B0495.6]	28	63	77	36	28
Trial 3					
wild type (N2)	91	-	-	100	100
apl-1(yn5)	92	-	-	45	40-50
yn38; apl-1(yn5)	85	-	-	100	90-100

yn38; apl-1(yn5); ynEx201 [TAG-235]	50	55	40	100	69
yn38; apl-1(yn5); ynEx202 [TAG-235]	109	70	62	87	61
yn38; apl-1(yn5); ynEx207 [DNJ-24]	85	69	49	100	62
yn38; apl-1(yn5); ynEx208 [DNJ-24]	80	72	34	76	60
yn38; apl-1(yn5); ynEx203 [R155.2]	124	61	16	46	66
yn38; apl-1(yn5); ynEx204 [R155.2]	74	84	33	49	53
yn38; apl-1(yn5); ynEx205 [R155.2]	157	57	22	49	68
yn38; apl-1(yn5); ynEx206 [R155.2]	98	68	48	71	63
yn39; apl-1(yn5)	114	-	-	11	10-20
yn39; apl-1(yn5); ynEx209 [B0495.6]	78	63	62	33	32
yn39; apl-1(yn5); ynEx210 [B0495.6]	30	67	42	17	33
yn39; apl-1(yn5); ynEx211 [B0495.6]	61	72	75	25	35

Formula to calculate the expected survival at 27^{o}C: (observed survival rate of *yn38* or *yn39* x (1- (GFP transmission rate at 20^{o}C) + ((GFP transmission rate at 20^{o}C) x (observed survival rate of *apl-1(yn5)*). P*myo-3*::mCherry was used as a co-injection marker for the transgenic strains.